Paleoceanography and Paleoclimatology

AGU ADVANCING EARTH AND SPACE SCIENCE

RESEARCH ARTICLE
10.1029/2022PA004550

A Window Into Eastern Mediterranean Productivity Conditions Over Three Pliocene Precession-Forced Climate Cycles

A. Cutmore[1], N. Bale[1], G. J. De Lange[2], I. A. Nijenhuis[2], and L. J. Lourens[2]

[1]Department of Marine Microbiology and Biogeochemistry, NIOZ Royal Institute for Sea Research, Den Burg, The Netherlands, [2]Department of Earth Sciences, Faculty of Geosciences, Utrecht University, Utrecht, The Netherlands

Key Points:

- The two Lido Rossello laminated layers are likely caused by an intermittently present dysoxic/anoxic pool which preserved organic material
- The laminated and gray marl layers offer rare insight into Early Pliocene eastern Mediterranean productivity during precession minimum/maximum
- Precession minimum, productivity dominated by shade-flora. Precession maximum, productivity composed of a spring-bloom and summer shade-flora

Supporting Information:

Supporting Information may be found in the online version of this article.

Correspondence to:

A. Cutmore,
anna.cutmore@nioz.nl

Citation:

Cutmore, A., Bale, N., De Lange, G. J., Nijenhuis, I. A., & Lourens, L. J. (2023). A window into eastern Mediterranean productivity conditions over three Pliocene precession-forced climate cycles. *Paleoceanography and Paleoclimatology*, *38*, e2022PA004550. https://doi.org/10.1029/2022PA004550

Received 21 OCT 2022
Accepted 1 APR 2023

The copyright line for this article was changed on 20 APR 2023 after original online publication.

Author Contributions:

Conceptualization: L. J. Lourens
Funding acquisition: L. J. Lourens
Investigation: A. Cutmore, G. J. De Lange, I. A. Nijenhuis, L. J. Lourens
Supervision: N. Bale, G. J. De Lange, L. J. Lourens
Writing – original draft: A. Cutmore

Abstract Here, we explore the importance of export productivity versus anoxia in the formation of sedimentary layers with enhanced total organic carbon (TOC) content. We use geochemical, sedimentological and micropaleontological records from two SW Sicily outcropping successions, Lido Rossello (LR) and Punta di Maiata (PM), over three Early Pliocene precession-forced climate cycles (4.7–4.6 million years ago [Ma]). Gray marls, deposited during precession minima, show enhanced TOC in both records. We suggest that basin-wide, low-oxygenated bottom-waters, resulting from freshwater-induced stratification during precession minimum, was integral to preserving gray marl TOC. Furthermore, prolonged eastern Mediterranean stratification may have produced a deep chlorophyll maximum (DCM), leading to "shade-flora" dominated productivity. The LR succession displays two unique laminated layers containing enhanced TOC. These laminations do not occur at specific times in the precession cycle or in time-equivalent PM samples. They are likely to have been produced by an intermittent dysoxic/anoxic pool at LR, caused by a local depression, which enhanced TOC preservation. Consequently, the laminations provide a rare window into "true" eastern Mediterranean productivity conditions during precession maxima, as organic matter is typically poorly preserved during these period due to enhanced ventilation. The laminated "windows" indicate that eastern Mediterranean export productivity may not have been significantly lower during precession maxima compared to precession minima, as previously thought. During these periods, productivity conditions are likely to have been comparable to the modern eastern Mediterranean, with a spring-bloom caused by enhanced winter/spring deep-water mixing preceding a summer "shade-flora" bloom caused by a summer-stratification induced DCM.

1. Introduction

Periodic discrete layers of black, organic-rich material, known as sapropels, are found in eastern Mediterranean sedimentary sequences throughout the Neogene and Quaternary (Hilgen et al., 2003; Kullenberg, 1952; Olausson, 1961; Rossignol-Strick et al., 1982; Vergnaud-Grazzini et al., 1977). These layers are associated with an enhanced freshwater influx into the eastern Mediterranean, linked to precipitation intensification in circum-Mediterranean regions (Rohling et al., 2002; Rohling & Hilgen, 1991; Rossignol-Strick, 1983, 1985; Scrivner et al., 2004; Wu et al., 2018). These climate conditions are predominately related to the Milankovitch precessional cycle, whereby perihelion occurs in Northern Hemisphere summer (every ~21 thousand years [ka]) (Rohling & Hilgen, 1991; Rossignol-Strick, 1983, 1985). This enhanced freshwater-input lowers the surface-water salinity and causes stratification in the eastern Mediterranean (Rohling & Hilgen, 1991; van der Meer et al., 2007). The underlying mechanism causing sapropel formation, however, is still debated, giving rise to a contentious debate over the relative importance of export productivity (Calvert, 1983) versus stratification-driven anoxia (Olausson, 1961).

Several suggestions have been proposed for the cause of enhanced primary productivity: (a) a reversal in the vertical flow of nutrient-poor surface-waters and nutrient-enriched deep-waters (Calvert, 1983; Calvert et al., 1992); (b) an increased nutrient supply from enhanced fresh-water runoff (Calvert, 1983); and (c) the development of a deep chlorophyll maximum (DCM) (Rohling & Gieskes, 1989). A DCM develops in stratified regions of the Mediterranean where the freshening of Mediterranean intermediate water at its source in the Levantine basin causes a shoaling of the pycnocline. This leads to an overlap between the pycnocline/nutricline and the base of the euphotic zone, producing a DCM (Rohling & Gieskes, 1989). The DCM scenario as locus for enhanced export production during sapropel formation has been favored by microfossil studies of foraminifera (Corselli et al., 2002;

Writing – review & editing: A. Cutmore, N. Bale, G. J. De Lange, I. A. Nijenhuis, L. J. Lourens

Lourens et al., 1992; Rohling & Gieskes, 1989), calcareous nannofossils (Castradori, 1993; Corselli et al., 2002), diatoms (Corselli et al., 2002; Kemp et al., 1999), and nitrogen isotope measurements of fossil chlorophyll (Sachs & Repeta, 1999).

Calculations based on a simple two-layered ocean model for the Mediterranean show that the permanent pycnocline between intermediate and surface-waters may have shoaled into the euphotic zone at times of sapropel formation resulting from reduced surface-water salinities (Rohling, 1991). This process would not only account for the incursion of nutrient-enriched intermediate water into the photic zone to fuel new production by a deep-dwelling algal community, but also reduce ventilation of the deep-waters, thereby facilitating anoxic conditions down from a few hundred meters in the water column (Rohling, 1994). In some highly organic-rich sapropels of Pliocene age, derivatives of isorenieratene were found, indicating that anoxic conditions may have extended into the lower euphotic zone (Passier et al., 1999).

Focusing on samples from a unique setting in Sicily (Figure 1), we aim to explore preservation and productivity changes in the eastern Mediterranean over three Pliocene (5.3–2.6 Mya) precession-forced climate cycles. Using geochemical, micropaleontological and sedimentological records, we aim to (a) better understand the relative role of enhanced productivity versus stratification-driven anoxia in the formation of sedimentary layers with enhanced organic carbon content, and (b) explore the contribution of a DCM to primary productivity in the eastern Mediterranean during periods of precession minima and precession maxima.

2. Environmental Setting

2.1. Geological Setting

Over 4 km of exposed marine Pliocene sediments can be found as continuous cliff outcrops along the south Sicily coastline. These outcrops cover the lower Pliocene "Trubi" formation with these sediments formed at a 500–800 m water depth (Brolsma, 1978).

The Pliocene Trubi formation sediments show a quadripartite cycle of white limestone, gray marl, white limestone, beige marl, reflecting productivity changes resulting from changing cyclicity (Brolsma, 1978). While the gray marl sediments cannot be strictly defined as sapropels, as their total organic carbon (TOC) content does not exceed 2% (Calvert, 1983), these layers are slightly TOC-enriched (0.1%–1.2%) comparative to the white and beige layers (Van Os et al., 1994) and coincide with minimum precession (i.e., Northern Hemisphere summer insolation maximum). These layers are therefore useful for better understanding the processes responsible for sapropel formation.

For this study, Pliocene Trubi sediment samples were taken from two locations of this outcrop: Lido Rossello (LR) and Punta di Maiata (PM), located <2 km apart (Figure 1). Both span carbonate cycles 29, 30 and 31 of the Trubi Formation (4.7–4.6 million years ago [Ma]), defined by Hilgen and Langereis (1989). What makes these records of particular interest is the presence of two intercalations of brownish-rose, finely laminated diatomaceous-enriched limestone layers in the LR record that are not observed in the time-equivalent PM samples (Brolsma, 1978). The laminated layers' presence at LR and absence at PM provides the opportunity to compare differences in paleoceanographic conditions and diagenetic processes between both localities in order to shed new light upon the climatic mechanisms causing the astronomically-driven carbonate cycles (Hilgen, 1991; Lourens et al., 1996).

2.2. Oceanographic Setting

The Mediterranean Sea has been an elongated satellite basin of the Atlantic since at least the late Miocene (Rögl & Steininger, 1983). The modern Mediterranean is extremely oligotrophic (Azov, 1986; Berman, Azov, et al., 1984; Berman, Townsand, et al., 1984; Krom et al., 1991) and its hydrography is dominated by three water masses: Modified Atlantic Water, found at the surface (50–200 m); Levantine Intermediate Water (200–800 m); and Mediterranean Deep Water, formed in both western and eastern basins (Lacombe & Tchernia, 1972; Wüst, 1960). In the eastern Mediterranean, evaporation is dominant over freshwater-input leading to high-salinity waters which contrast with the inflowing lower salinity Atlantic waters in the western basin. This forms a west to east salinity gradient, driving an anti-estuarine circulation pattern (Wüst, 1960). This large-scale circulation system has been present since the end of the Messinian age (5.33 Ma), although during the Pliocene, the west to east salinity

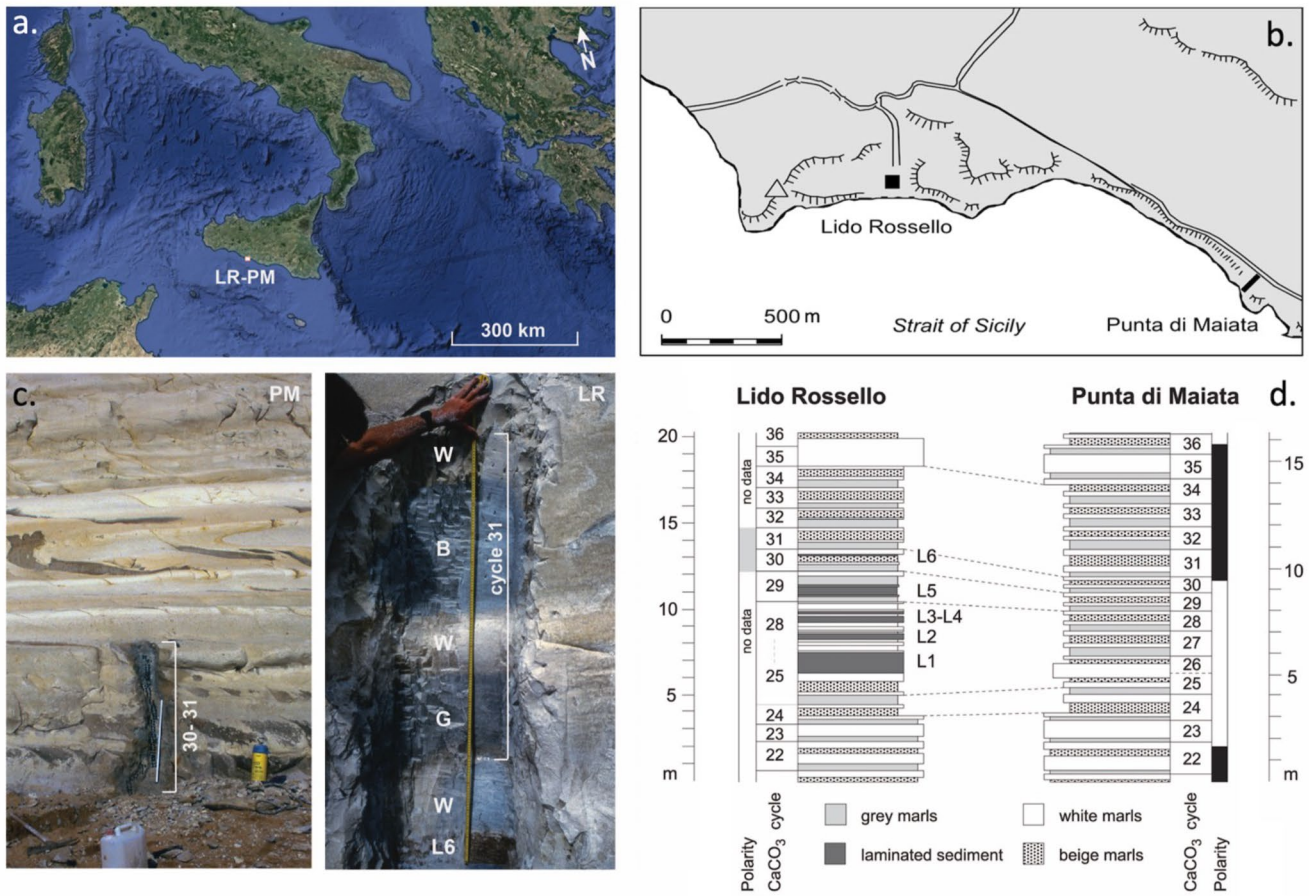

Figure 1. (a and b) Map showing the two locations from which samples of the Pliocene Trubi sediments were taken: Lido Rossello (LR) and Punta di Maiata (PM). Both records span three carbonate cycles (29, 30 and 31) of the Trubi Formation; (c) Photograph of quadripartite carbonate cycles in the LR and PM outcrop successions; (d) Depth of carbonate cycles 22–36 in the LR and PM records, illustrating the quadripartite layers and position of the laminated layers within the LR record.

gradient was significantly lower than present day and sea surface temperatures were higher (Beltran et al., 2021; Thunell, 1979).

Today, there is a large seasonal contrast in water temperatures and vertical mixing of the surface-waters in the Mediterranean (Marullo et al., 1999). During winter, (semi-) permanent eddies in the east (Levantine basin), and deep turbulent mixing or mesoscale cyclonic and anticyclonic gyres in the west (Ionian basin), fertilize surface-waters and cause a deep mixed-layer (Brenner et al., 1991). This leads to enhanced productivity at the surface and a "spring-bloom" (Krom et al., 1992; Ziveri et al., 2000). In the Ionian Basin this "spring-bloom" is dominated by a high abundance of coccolithophores, diatoms and dinoflagellates (Malinverno et al., 2003, 2014; Varkitzi et al., 2020) and a high standing-stock of the planktonic foraminiferal species *Globigerina bulloides*, *Globigerina inflata*, and *Globorotalia truncatulinoides* (Pujol & Vergnaud-Grazzini, 1995), which primarily depend on deep convective overturning for their lifecycle (Reichart et al., 1998). In summer, the photic zone becomes well-stratified leading to highly oligotrophic conditions in the shallow mixed-layer (~25 m), and eutrophic conditions associated with a DCM at the seasonal thermocline and/or pycnocline (Pujol & Vergnaud-Grazzini, 1995; Roussenov et al., 1995). Primary productivity in the eastern Mediterranean at this time is dominated by "shade-flora" (primarily diatoms) which regulate their buoyancy to move between the euphotic zone and a deeper nutrient source and/or have adapted to low-light conditions (Kemp et al., 1999, 2000). In autumn, the breakdown of summer-stratification causes a "dump" of these shade-flora to the sea-floor (Kemp et al., 2000). Although the growth rate and primary production of "shade-flora" is typically lower than the spring-bloom, the total primary production of summer phytoplankton can be equal to/greater than the spring-bloom, as it occurs over several summer months (Kemp et al., 2000).

3. Materials and Methods

3.1. Sampling

Samples from LR and PM were taken over three campaigns: October 1994, June 1995, and August 1996. Prior to sampling, the weathered surface was removed to expose fresh sediment. Small cores (2.5 cm diameter, 8 cm length) were horizontally drilled and packaged in aluminum foil. During the 1994 campaign, additional samples for geochemical analysis were removed parallel to the bedding plane using a stainless-steel spatula and placed in small glass jars. All other geochemical analysis was performed on 5 mm samples scraped off of the drilled cores.

3.2. Geochemical Analyses

Freeze-dried sediments were ground in an agate mortar mill and analyzed for TOC, total organic nitrogen (TON) using a ThermoScientific Flash EA Delta V Plus IRMS. Temperature for oxidation, reduction and the oven were 900, 680, and 40°C, respectively. Flow was 100 ml/min. Prior to TOC analysis, inorganic carbon was removed from the sediment using HCl (2 mol), cleaned with bi-distilled water, then freeze-dried. Opal analyses were performed on selected samples, following the method of Müller and Schneider (1993), using a Technicon TRAACS 800 auto-analyzer. A subsample (~250 mg) was digested in hydrofluoric acid (10 ml; 40%) and a 10 ml mixture (6.5:2.5:1) of $HClO_4$ (60%), HNO_3 (65%) and H_2O at 90°C. After evaporation of the solutions (190°C on a sand bath), the dry residue was dissolved in 50 ml 1 M HCl. The concentration of elements Ba, Al, P, S, Fe, Mo, Ti, V, Sc and other various trace elements were measured with an inductively coupled plasma emission spectrometer (ICP-AES: Perkin Elmer Optima 3000) and are expressed in % or parts per million (ppm). The analytical precision and accuracy were determined by replicate analyses of samples and by comparison with international (BCR-71) and in-house (F-TURB and MM-91) standards. Relative standard deviations, analytical precision, and accuracy were better than 3%. Bulk $CaCO_3$ content was derived from the % weight of Ca which was obtained through ICP-AES. These analyses were performed at the University of Utrecht, GeoLab.

Biogenic barium (Ba_{bio}) is a useful proxy of export productivity, defined as the fraction of total Ba not associated with terrigenous material (Calvert, 1983; Paytan & Griffiths, 2007; Schoepfer et al., 2015), calculated using the element's total flux, the sample's Al content, and the ratio of terrigenous Ba/Al ($(Ba/Al)_{terrigenous}$).

$$Ba_{bio} = Ba_{total} - Al * (Ba/Al)_{terrigenous}$$

An average $(Ba/Al)_{terrigenous}$ value of ~0.0019 was derived from the beige intervals by assuming ~70% of the Ba within these intervals comes from Saharan dust (Van Os et al., 1994).

3.3. Isotope Analyses

The $\delta^{13}C$ and $\delta^{18}O$ of two planktonic foraminiferal species (*Globigerinoides obliquus* [Bolli] and dextrally-coiled *Neogloboquadrina acostaensis* [Blow]) and one benthic species (*Cibicidoides italicus* [di Napoli]) were measured at the University of Utrecht, GeoLab. Approximately 60 specimens of *G. obliquus* and ~100 specimens of *N. acostaensis* were picked per sample (104 LR samples and 77 PM samples) from the 125–595 µm fraction, with ~3 *C. italicus* specimens picked per sample (72 LR samples and 39 PM samples) in the >212 µm size range. In several samples of the two sections, the size of all specimens of both planktonic species were measured to check the size variability. These measurements indicate that the average size and standard deviation for the various samples are nearly identical, with an average size of ~310 ± 50 µm and ~205 ± 30 µm for *G. obliquus* and *N. acostaensis*, respectively. Consequently, we assume that the picked specimens for isotopic measurement are from the same size range.

To remove any organic remains, the picked planktonic foraminifera were heated for 30 min at 470°C under vacuum. Parts of the samples were transferred into glass reaction tubes and evacuated for 14 hr, followed by 6 hr of reaction with 103% phosphoric acid at 25°C under high vacuum. The released CO_2 was cryogenically separated from other gases and measured on a VG SIRA 24 mass spectrometer. The remaining planktonic samples were analyzed using an ISOCARB directly coupled to the mass spectrometer, reacting with 103% phosphoric acid for 6–7 min at 90°C. Samples were run alongside one international (IAEA-CO-1) and nine in-house (NAXOS) standards. During each run a linear decrease in the isotopic composition of the NAXOS standards was observed, which varied between 0.05 and 0.2, and 0.1 and 0.4‰ for $\delta^{13}C$ and $\delta^{18}O$ respectively. This linear trend is likely

related to an increase in the phosphoric acid concentration due to water loss during the analyses, therefore a (linear) correction of the samples was applied using the NAXOS standard as reference. The analytical precision and accuracy were determined by replicate analyses of samples and by the comparison with international (IAEA-CO-1 and NBS-19) standards, with the relative standard deviations, analytical precision, and accuracy better than 0.05 and 0.1‰ for $\delta^{13}C$ and $\delta^{18}O$ respectively. The benthic foraminiferal specimens were ultrasonically cleaned and analyzed with an automated carbonate reaction device (Kiel III) coupled to a Thermo-Finnigan MAT253. Each sample reacted with 103% phosphoric acid (H_3PO_4) for 7 min at 70°C. Calibration to the international carbonate standard NBS-19 revealed an analytical precision better than 0.1 and 0.03‰ for $\delta^{13}C$ and $\delta^{18}O$, respectively. All data are reported as per mil (‰) relative to the VPDB standard.

3.4. Micropalaeontological Analyses

200–400 planktonic foraminiferal specimens were picked from the 125–595 µm size fraction (101 LR samples and 49 PM samples). These were mounted on Chapman slides, identified and counted. For each slide, benthic foraminifera, siliceous organisms and palynomorphs were also counted. In some samples, organic compounds of small spherical objects (always wrinkled) were observed. Brolsma (1978) had these forms tentatively identified by G.T. Boalch (Plymouth) as possible representatives of the genus *Pachysphaera* (division Chlorophyta [green algea], class Prasinophyceae [Boalch & Parke, 1971]). In this study, these components have been combined into one category: prasinophytes.

The planktic foraminifera ratio was calculated as follows: planktonic count/(benthic + planktonic counts). Micropalaeontological records are presented here using mass accumulation rates (# cm^{-2} yr^{-1}), calculated using the counts per gram of dry sediment, the sedimentation rate (ka cm^{-1}), and dry bulk density (ρ) (g cm^{-3}) of the sample.

4. Results

4.1. Astronomical Tuning and Phase Relations

As starting point for our chronology, astronomical ages for the midpoints of the gray layers of PM have been taken from Lourens et al. (1996). These astronomical ages refer to 3-ka lagged ages of the correlative maxima in the $La90_{(1,1)}$ summer insolation curve. Additionally, the cyclic variations in the Ti/Al ratio of marine sediments in the Mediterranean can be used to refine the astronomical age model within one cycle, due to the approximately linear response of this proxy to changes in summer insolation (Lourens et al., 2001). From a detailed comparison between the Ti/Al record of Ocean Drilling Program 967 spanning 2.4–2.9 Ma and the La90 solution (Laskar et al., 1993), Lourens et al. (2001) obtained the optimum fit for all La90 solutions including values for the dynamical ellipticity and/or tidal dissipation (with respect to their present-day estimates) ranging from 1.003 and 0 to 0.9997 and 1, respectively. The observed smaller average value for the combined dissipative effects was attributed to the severe glacial cyclicity, which harassed global climate over the last 3 Ma. Presently, it is still unclear if this relationship also holds true for the early Pliocene since large ice caps were absent during that time interval. For the present study the $La90_{(1,1)}$ summer insolation curve is maintained as target, because this solution yields on average the best fit with the geological record over the last 5.3 Ma (Lourens et al., 1996). Subsequently, our age model is refined for LR and PM by assigning the astronomical ages for maxima and minima in the Ti/Al ratio to their corresponding minima and maxima in the 65°N summer insolation curve (Figure 2). For ease of reference, a 3-ka time lag was not included as was proposed by Lourens et al. (1996).

Additional support for our age model comes from the good agreement between successive high and low amplitude Ti/Al maxima and the precession-obliquity interference patterns displayed in the summer insolation minima of insolation cycles 443–447 (see also Lourens et al., 1996). This interference is also clearly reflected in the lithological column of PM by a thick-thin-thick alternation of the beige layers. The good similarity between the age models of LR and PM and the quadripartite layering of the Trubi marls is corroborated by the $CaCO_3$ timeseries of both sections (Figure 2).

The gray marls are marked by slightly reduced dry bulk density (ρ), probably due to the more clayey character of the sediment (Figure 2). The two laminated beds (L5 and L6) are well expressed by very low ρ values. A thin homogeneous marly interval within L5 is indicated by a small ρ increase. From Figure 2 it is evident that these

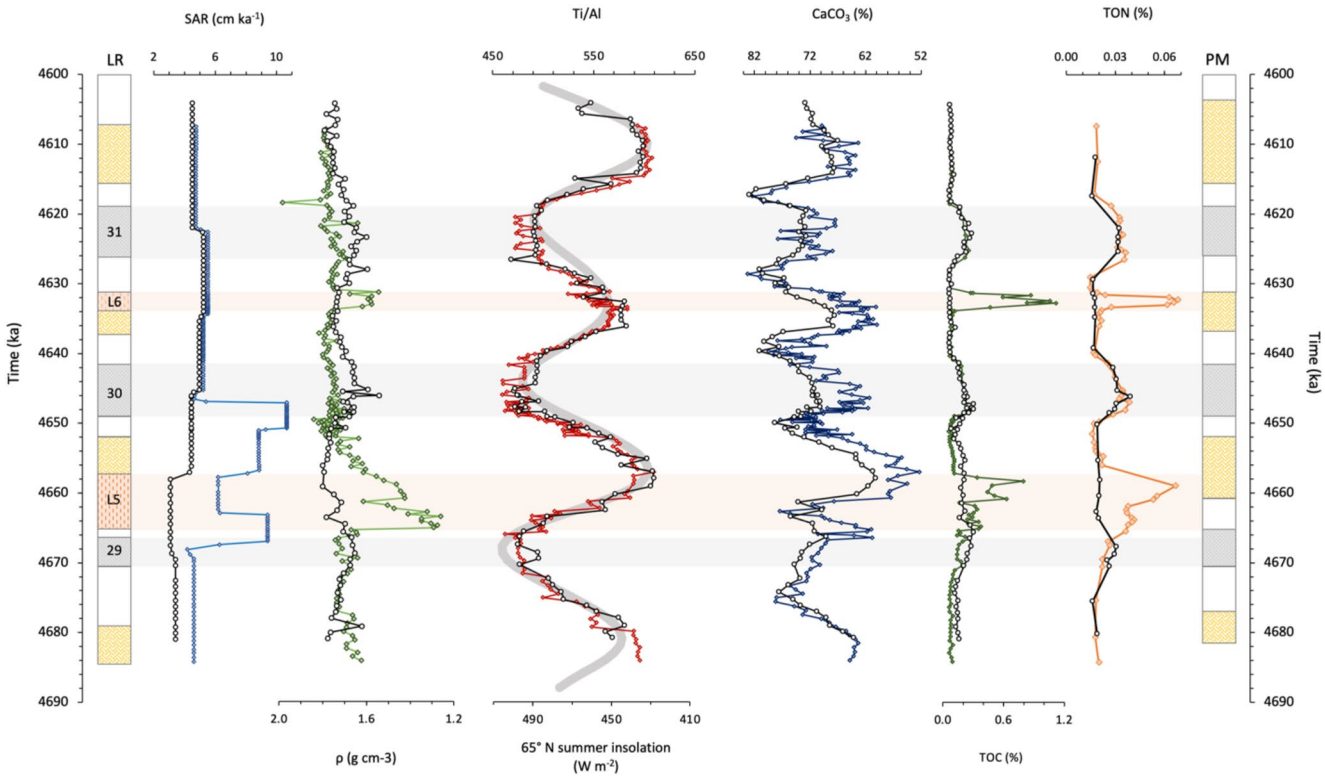

Figure 2. Changes, over three precession forced climate cycles (4,690–4,600 ka), in: sediment accumulation rate (SAR; cm ka^{-1}); dry bulk density (ρ) (g cm^{-3}); Ti/Al; $CaCO_3$ (%) note reverse scale; total organic carbon (TOC) (%); total organic nitrogen (TON) (%) in the SW Sicily records of Lido Rossello (LR) (colored lines with filled diamond markers) and Punta di Maiata (PM) (black lines with open circle markers). Change in summer insolation at 65°N (gray line; Berger & Loutre, 1991). On the left of the diagram, the layers associated with the three precession cycles (29, 30, 31) are shown and labeled, with gray bands depicting periods of precession minima. The laminated intervals (L5 and L6) of the LR record are labeled in the orange boxes and depicted by the orange bands.

two laminates are not related to a specific orbital configuration; L6 occurs slightly after a summer insolation minimum (i.e., transition from top beige to base white of cycle 30), while L5 coincides with the transitional interval from a summer insolation maximum to a minimum (i.e., top of gray to mid beige of cycle 29). This is in contrast with the gray-colored marls and associated minima in Ti/Al, which are ultimately-controlled by the astronomical (e.g., summer insolation maxima) perturbations (Lourens et al., 1996, 2001).

4.2. $CaCO_3$, TOC and TON

The characteristic quadripartite-layering of the Trubi Formation (De Visser et al., 1989) is clearly indicated by the fluctuations in carbonate content of both the studied sediment records, notwithstanding the exceptional occurrence of the laminated intervals in the LR record (Figure 2). $CaCO_3$ concentrations are enhanced in the white layers, have intermediate values in the gray layers and are lowest in the beige layers. The LR carbonate record does not display an aberrant pattern related to the laminated intervals L5 and L6. In both records, TOC and TON content is lowest in the white and beige layers (~0.08% and ~0.02%, respectively) and more enriched in the gray layers (up to 0.30% and 0.04%, respectively) (Figure 2). In the LR record, the highest values of TOC and TON are found in L5 (up to 0.80% at 4,658 ka, and 0.07% at 4,659 ka, respectively) and L6 (up to 1.12% at 4,633 ka, and 0.07 at 4,632 ka, respectively); these values are comparable to those found in the sapropels of the overlying Narbonne Formation (Van Os et al., 1994).

4.3. Trace Elements, Opal and Siliceous Organisms

The concentration of opal in the LR record peaks in the lower section of L5, reaching 4% at 4,665 ka. Ba_{bio} records from both sites show enhanced concentrations within all gray marls (Figure 3). In the laminated layers L5 and L6, Ba_{bio} concentrations increase. The largest Ba_{bio} increase occurs in the early part of L5, reaching ~800 ppm between 4,665 and 4,663 ka, which is coeval with a peak in the concentration of molybdenum (Mo)

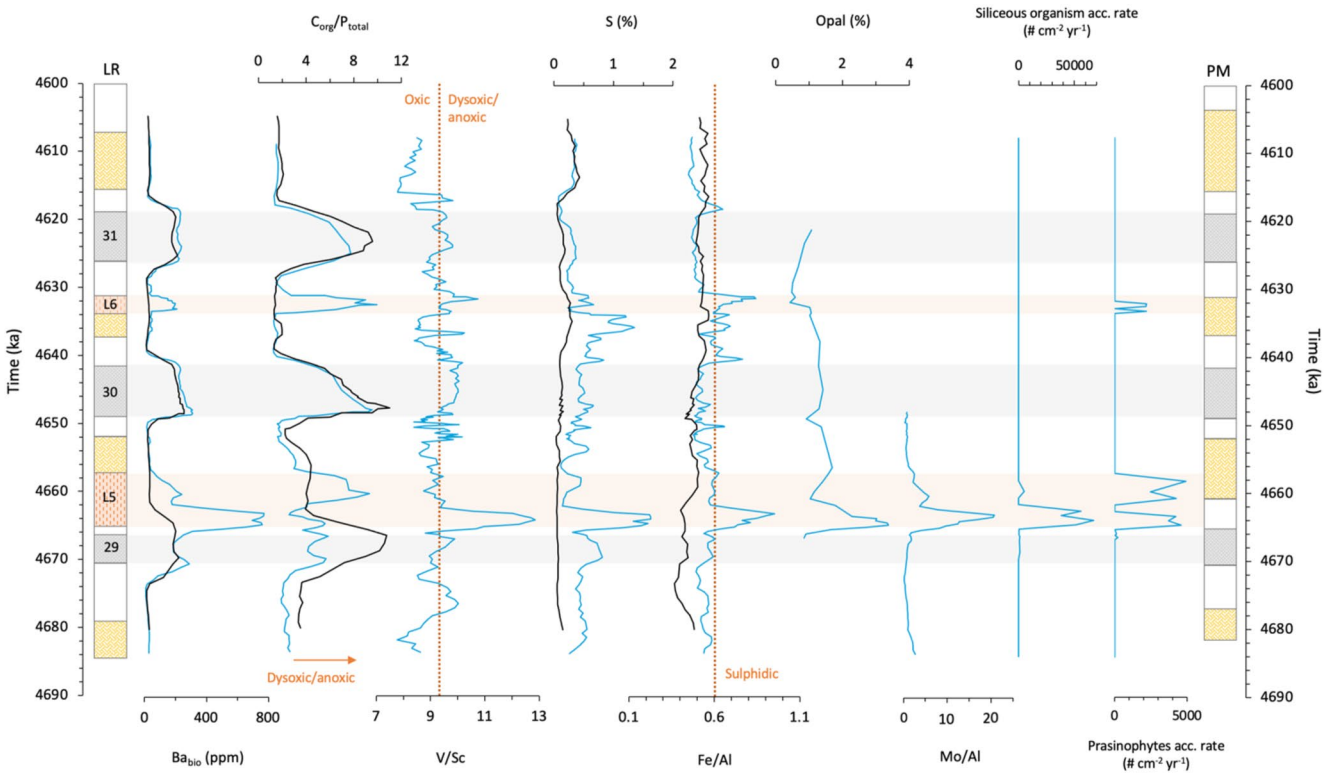

Figure 3. Changes, over three precession forced climate cycles (4,690–4,600 ka), in: Ba_{bio} (ppm); C_{org}/P_{total}; V/Sc; Sulfur (%); Fe/Al; Opal (%); Mo/Al; Siliceous organism acc. rate (# cm^{-2} yr^{-1}); Prasinophyte acc. rate (# cm^{-2} yr^{-1}); in the SW Sicily records of Lido Rossello (LR) (blue lines) and Punta di Maiata (PM) (black lines). All elements and ratios are displayed using a 3-point moving average.

(Figure 3). Siliceous organisms (radiolarians, diatoms and silicoflagellates) were found in the L5 interval (see also Zachariasse et al., 1978), reaching a peak of 67,215 organisms cm^{-3} yr^{-1} at 4,664 ka (Figure 3). The vanadium to scandium ratio (V/Sc) in the LR record shows higher values in the gray marls (~10) and in the laminated layers (~10 during L6, ~12 in the early part of L5, lowering to ~9 later in L5), and lower values in the beige and white layers (~8) (Figure 3). The ratio of organic carbon to total phosphorus (C_{org}/P_{total}) is also higher in the gray marls (~9) and the laminated layers (~8). The ratio of iron to aluminum (Fe/Al) is consistently low throughout the PM record (~0.5), which is also seen in the LR record, with the exception of slight increases during L6 and the start of L5, with peaks of ~0.9.

4.4. Prasinophytes (Green Algae)

In both L5 and L6, high abundances of the prasinophyte *Pachysphaera* and some large (>125 μm) phycomas of *Pterosperma* (Pouchet) spp. (also of the class Prasinophyceae) were found. Similar to *Halosphaera*, these green algae are pelagic organisms with a vegetative (motile) and an encysted (non-motile) stage (Boalch & Parke, 1971) and are very resistant to chemical or biological degradation (Wall et al., 1977). The few relevant literature sources on modern prasinophycean algae (*Pachysphaera*, *Halosphaera*, and *Pterosphaera*) and their fossil equivalents (*Tasmanites* and *Leiosphaeridia*) (Boalch & Parke, 1971; Guy-Ohlson, 1988) suggest they primarily occur in marine surface-waters of relatively high northern latitudes (cold) and epicontinental (fresh-water), often near-shore environments including the Mediterranean Sea (Prauss & Riegel, 1989). The prasinophyte *Halosphaera* has, however, been recorded at depths up to 1,000 m in the Mediterranean Sea and found living together with diatoms in deep-water algal communities (Kimor & Wood, 1975; Sournia, 1982). Their abundance at these depths is highest in autumn, with these organisms rising from deeper to surface-waters during winter and early spring (Jenkinson, 1986; Parke & Hartog-Adams, 1965).

4.5. Calcareous Organisms

Planktonic foraminiferal shells are well preserved in both records (as shown by scanning electron microscope images of various species of foraminifera from the Trubi Formation records; Figure S1 in the Supporting

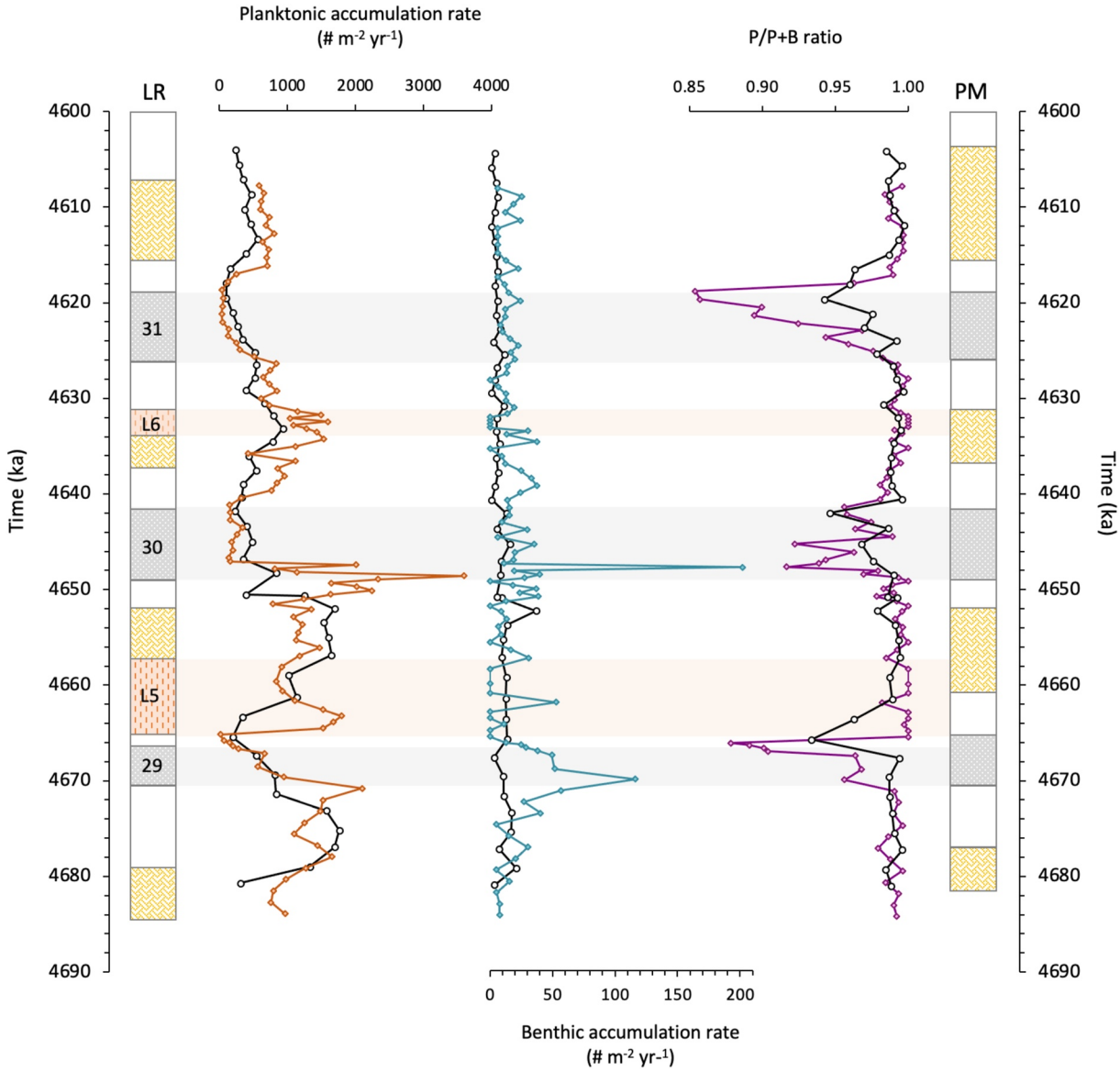

Figure 4. Changes, over three precession forced climate cycles (4,690–4,600 ka), in: planktonic foraminifera accumulation rate (# m^{-2} yr^{-1}); benthic foraminifera accumulation rate (# m^{-2} yr^{-1}); and P/P + B ratio; in the SW Sicily records of Lido Rossello (LR) (colored lines with filled diamond markers) and Punta di Maiata (PM) (black lines with open circle markers).

Information S1) and the identified species/groups are outlined in Table S1 in the Supporting Information S1. The relative abundance patterns of the various species display almost identical patterns in both records (Figure S2 in the Supporting Information S1), with small offsets which are attributed to differences in sample resolution. *Globoturborotalita apertura*, *Globigerina falconensis*, and dextrally-coiled *N. acostaensis* are the dominant species, followed by *Globigerinita glutinata* and *G. obliquus*. The less frequently occurring species *Sphaeroidinellopsis seminulina-subdehiscens*, *Globorotalia margaritae* and *Globigerinoides trilobus* appeared to be very useful for confirming the time correlations between LR and PM. *Turborotalita quinqueloba*, *Orbulina universa* and *Globigerinella siphonifera* are reflected by very low percentages. During deposition of the gray layers, sinistrally coiled *N. acostaensis* becomes more abundant relative to its dextrally coiled counterpart. Similar patterns were previously observed within the Trubi marls (De Visser et al., 1989).

The planktonic foraminiferal accumulation rate (# m^{-2} ka^{-1}) indicates that the flux of all species declined significantly during deposition of the gray layers but remained high within the beige and white layers (Figure 4). There is an increased accumulation rate of planktonic foraminifera in L6 and at the base of L5. The benthic foraminiferal

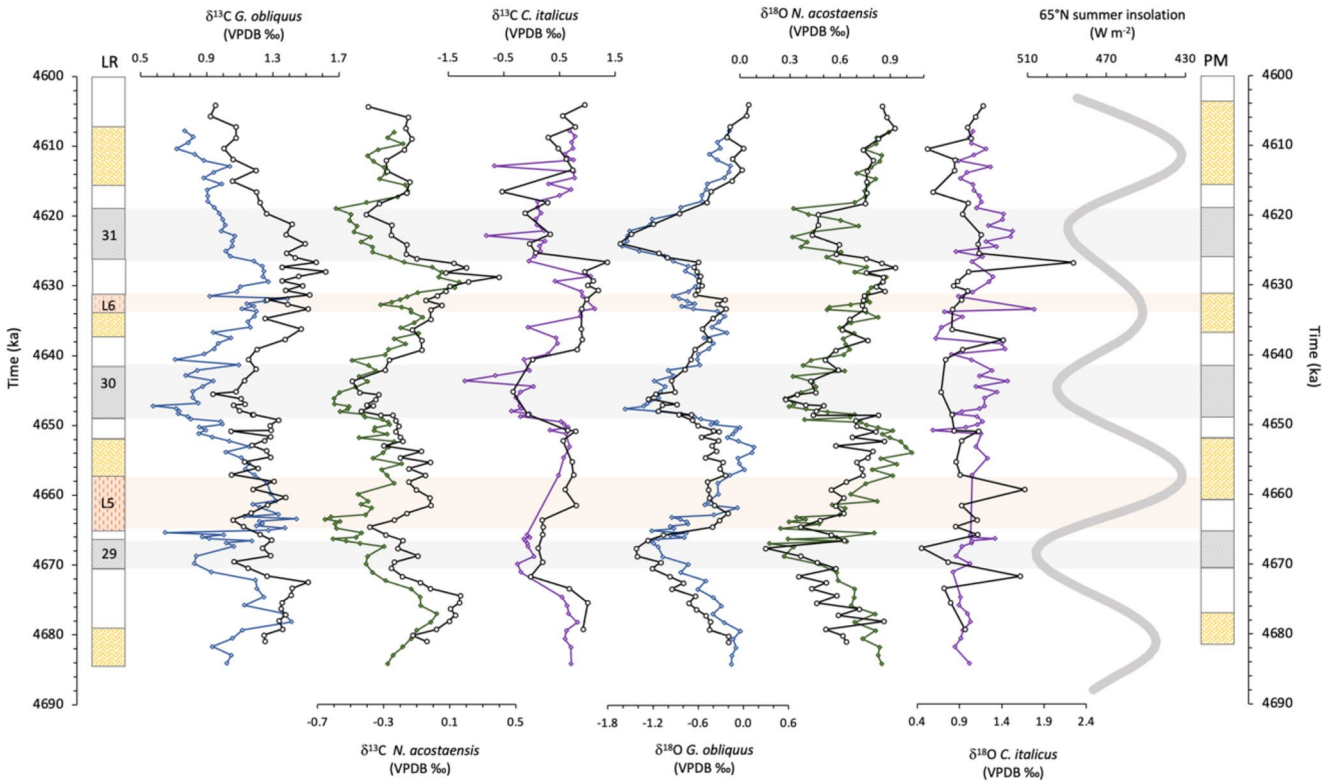

Figure 5. Changes, over three precession forced climate cycles (4,690–4,600 ka), in: $\delta^{13}C$ *Globigerinoides obliquus* (VPDB ‰); $\delta^{13}C$ *Neogloboquadrina acostaensis* (VPDB ‰); $\delta^{13}C$ *Cibicidoides italicus* (VPDB ‰); $\delta^{18}O$ *G. obliquus* (VPDB ‰); $\delta^{18}O$ *N. acostaensis* (VPDB ‰); $\delta^{18}O$ *C. italicus* (VPDB ‰) in the SW Sicily records of Lido Rossello (LR) (colored lines with filled diamond markers) and Punta di Maiata (PM) (black lines with open circle markers).

flux is low and remained rather constant throughout the studied interval and consequently, drops in the P/P + B ratio within the gray layers must be related to the significant decline in the amount of planktonic foraminiferal shells (Figure 4).

Preliminary nannofossil counts on the samples of LR cycles 29 and 30 shows that the coccoliths are overall not well preserved and are not very diverse (L. Beaufort, personal communication, 1996). Highest abundances were found for the white layers (not shown).

4.6. Stable Isotopes of Planktonic Foraminifers

The two planktonic foraminiferal species investigated for their stable isotopic composition, *G. obliquus* and dextrally-coiled *N. acostaensis*, were present throughout both records. *G. obliquus* is a mixed-layer, oligotrophic, warm water species, and its abundance in the Mediterranean gradually declined during the Plio/Pleistocene (Lourens et al., 1992, 1996) before becoming became extinct (Berggren & Amdurer, 1973; Parker, 1973). All living representatives of *Neogloboquadrina* belong to one biogeographic cline (Srinivasan & Kennett, 1976), which feed exclusively on phytoplankton (Hemleben et al., 1989) near or below the (seasonal) thermocline (~25–100 m) in association with maximum chlorophyll concentrations (Fairbanks et al., 1982; Ravelo & Fairbanks, 1992). In the present-day eastern Mediterranean, *N. pachyderma* (dex) occurs in low abundances and in some areas it might be associated with a DCM (Dowidar, 1984). We assume that *N. acostensis* (dex) had a similar feeding strategy to its modern representatives, inhabiting the thermocline in seasonally productive regions (Lourens et al., 1992). The benthic foraminifera species investigated for its stable isotopic composition, *C. italicus*, is an epifaunal species endemic to the Mediterranean basin, living at the sediment surface (Sprovieri & Hasegawa, 1990).

At both sites, the $\delta^{18}O$ records of both planktonic species display a similar pattern and values (Figure 5). The $\delta^{18}O$ record of both species closely follow Northern Hemisphere summer insolation (65°N): minimum $\delta^{18}O$ coincide

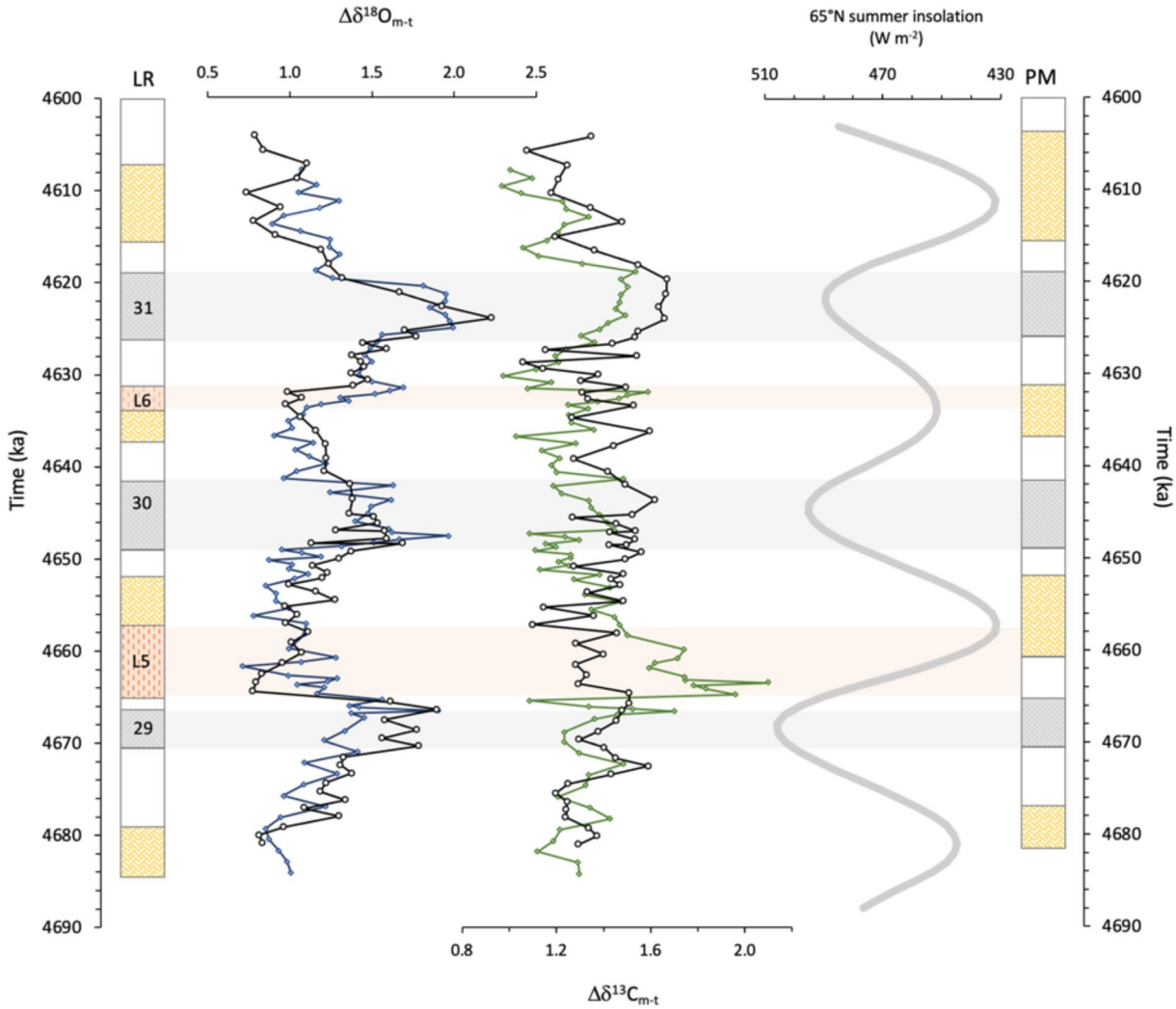

Figure 6. Changes, over three precession forced climate cycles (4,690–4,600 ka), in: the oxygen isotope difference between the mixed-layer and the thermocline ($\Delta\delta^{18}O_{m\text{-}t}$; VPDB ‰); the carbon isotope difference between the mixed-layer and the thermocline ($\Delta\delta^{13}C_{m\text{-}t}$; VPDB ‰); in the SW Sicily records of Lido Rossello (LR) (colored lines with filled diamond markers) and Punta di Maiata (PM) (black lines with open circle markers). Change in summer insolation at 65°N (gray line; Berger & Loutre, 1991).

with maximum summer insolation and gray layer deposition, while maximum $\delta^{18}O$ values coincide with minimum summer insolation and the beige layer deposition. While both records show similar patterns, the *G. obliquus* record shows more negative values (~−1.3‰) compared to *N. acostaensis*. This is in part caused by their different depth habitats and confirms the assumed vertical distribution pattern of both species within the photic zone (Williams et al., 1979). The covariation of these records suggests both species thrived at approximately the same time of the year, implying that their difference in oxygen isotope composition can be used to reconstruct variations in the thermocline structure (i.e., summer to autumn) (Ravelo & Fairbanks, 1992). The greatest oxygen isotope difference between the mixed-layer and the thermocline ($\Delta\delta^{18}O_{m\text{-}t}$), as shown by *G. obliquus* and *N. acostaensis*, occurs in the gray layers, while the beige layers display the smallest difference (Figure 6). Furthermore, $\Delta\delta^{18}O_{m\text{-}t}$ is similar at PM and LR, throughout the record.

The $\delta^{13}C$ records of both planktonic species display very similar patterns at both sites, with the exception of the laminated intervals L5 and L6 which show small negative excursions in *N. acostaensis* $\delta^{13}C$ (~−0.3‰). The $\delta^{13}C$ of both species, however, varies between the two sites; there is a systematic shift toward more positive values in the PM record compared to LR for both species (0.25 and 0.15‰ for *G. obliquus* and *N. acostaensis*, respectively). *N. acostaensis* $\delta^{13}C$ shows a very similar pattern to the insolation record, with minimum $\delta^{13}C$ coinciding with maximum summer insolation and gray marl deposition, and maximum $\delta^{13}C$ coinciding with

minimum summer insolation and beige layer deposition. *G. obliquus* $\delta^{13}C$ shows a similar relationship with summer insolation in the early part of both records, but this breaks down after ~4.62 Ma with $\delta^{13}C$ continuously declining until 4.60 Ma. Despite similar patterns in $\delta^{13}C$ of both planktonic species, *G. obliquus* displays more positive values (+1.3‰) than *N. acostaensis*, which is also likely the result of their different depth habitats (Kroopnick, 1985). The carbon isotope difference between the mixed-layer and the thermocline ($\Delta\delta^{13}C_{m\text{-}t}$), as shown by *G. obliquus* and *N. acostaensis*, varies throughout the record (Figure 6) with the smallest difference shown in the white layers and the largest difference occurring in L5 (~2.0‰), although this is not shown in the time-equivalent PM samples.

At both sites, $\delta^{13}C$ of benthic species *C. italicus* displays similar patterns, with a clear depletion in $\delta^{13}C$ in the gray layers (−1.0‰) compared to the rest of the timeseries (Figure 5). With regards to the stable oxygen isotope record of *C. italicus*, the two sites do not show a similar pattern. In the LR record, two carbonate cycles (30 and 31) display an increase in $\delta^{18}O_{C.\ italicus}$ in the gray layers. The PM record, however, shows no distinct pattern between the layers, but does generally display lower $\delta^{18}O_{C.\ italicus}$ values compared to that of the LR site (−0.3‰). The low-resolution of both the *C. italicus* $\delta^{18}O$ and $\delta^{13}C$ records in the laminated layers of the LR record prevent a thorough analysis of these intervals.

5. Discussion

5.1. Possible Causes of the Laminated Intervals at the LR Site

The two laminated diatomaceous-enriched limestone layers observed in the LR record are not present in the time-equivalent samples at PM. While L5 coincides with declining summer insolation (65°N) and the deposition of white and beige layers in the PM record, L6 coincides with minimum summer insolation (65°N) and the upper section of a beige layer in the PM record.

Sediments under high productivity areas are known to contain elevated concentrations of organic matter (Canfield, 1994; Pedersen & Calvert, 1990), biogenic and diagenetic phosphate (e.g., Burnett, 1977; Froelich et al., 1988), and barite-barium formed in micro-environments containing decaying organic matter (e.g., Bishop, 1988; Dehairs et al., 1980). Both laminated intervals are characterized by elevated concentrations of Ba_{bio} and TOC, indicating enhanced palaeo-productivity conditions during deposition of these layers (Schoepfer et al., 2015; Tribovillard et al., 2006). During L5, a localized increase in surface-ocean productivity and an intensified oxygen minimum zone below the surface may be inferred from the higher $\delta^{13}C$ values of surface-dwelling *G. obliquus*, lower values of thermocline-dwelling *N. acostaensis*, and consequently the enhanced carbon isotope gradient between the mixed-layer and thermocline ($\Delta\delta^{13}C_{m\text{-}t}$) (Figure 6) (Corfield & Cartlidge, 1992; Shackleton, 1985).

It is possible, however, that these primary productivity conditions occurred over the wider region and were preserved only at LR because of a local depression. Such a depression may have led to the intermittent presence of a stagnant dysoxic/anoxic pool at LR which contained high levels of dissolved silica and barium (Björklund & De Ruiter, 1987; De Lange et al., 1990; Erba, 1991). The preservation of opaline skeletons is a rare occurrence in Mediterranean sediments as these waters are highly undersaturated in silica (Kemp et al., 1999), but this dysoxic/anoxic pool may have acted as a geochemical buffer, leading to the preservation of siliceous skeletons as seen in L5 (Figure 3), and the enhanced preservation of opal, TOC and Ba_{bio} in both laminated layers. Redox-sensitive elements in the record are consistent with this theory. The first of these is V; the ratio of V/Sc is a useful proxy for bottom-water oxygen conditions, with values <9.1, as seen in our laminated intervals (Figure 3) indicating dysoxia/anoxia (e.g., Calvert & Pedersen, 1993; Emerson & Huested, 1991; Gallego-Torres et al., 2007). This is further supported by the presence of the redox-sensitive element Mo in L5 (Figure 3), which is found in higher concentrations in anoxic sediments (e.g., Algeo & Lyons, 2006; Calvert & Pedersen, 1993; Crusius et al., 1996; Emerson & Huested, 1991; Nijenhuis et al., 1999; Scheiderich et al., 2010). Finally, Fe/Al values >0.6 in the sedimentary record are interpreted as representing euxinic bottom-water conditions, whereby Fe_2^+ reacts with dissolved sulfide to form Fe sulfide minerals that are then preserved in the underlying sediments, leading to increased Fe/Al and S (Azrieli-Tala et al., 2014; Canfield et al., 1996; Lyons & Severmann, 2006; Scheiderich et al., 2010). This pattern is seen here in our LR records, with corresponding peaks in Fe/Al and S occurring in both laminated intervals and values of the former exceeding 0.6 (Figure 3). In the time-equivalent samples of the PM record, Fe/Al and S are significantly lower and do not show the same increase. This indicates that conditions

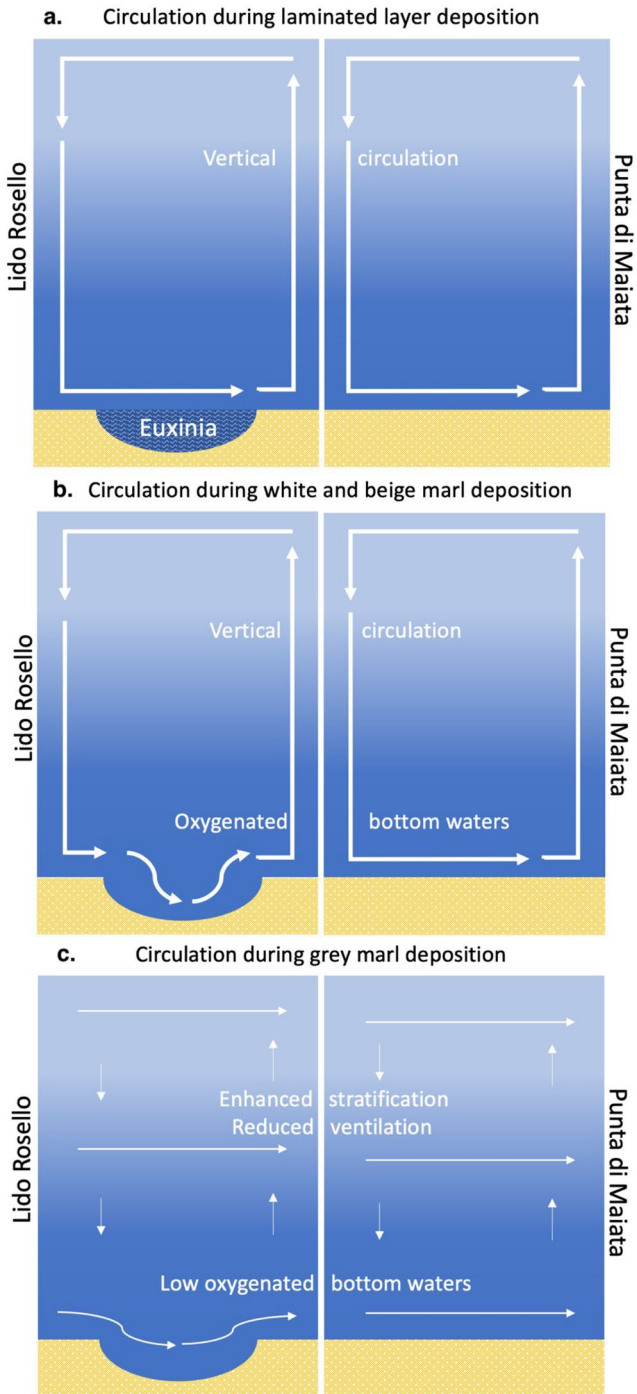

Figure 7. Illustration of the circulation changes during the deposition of different layers in both records, and the geological differences in the seafloor topography at the Lido Rossello and Punta di Maiata sites.

in the LR depression may have been euxinic as well as dysoxic/anoxic during the deposition of the laminated sediments.

A slump level directly below the first laminated interval (Brolsma, 1978) possibly reflects the formation of a small physical depression at the LR site. It is possible that while this depression was present at LR throughout this period, local bottom-water circulation patterns determined the oxygenation of this pool. During the deposition of the laminated layers, it is possible that localized changes led to poor ventilation in the pool, causing anoxic, sulfidic conditions, despite a well-ventilated water column above (illustrated in Figure 7a). The absence of benthic organisms in both laminated layers of the LR record, but their presence during the same period of the PM record also indicates dysoxic/anoxic conditions at LR. At PM, bottom-waters at these times are likely to have been well-oxygenated and undersaturated with respect to barium and silica, shown by the lower concentrations of TOC and Ba_{bio} and absence of siliceous opaline skeletons. Considering the sediment accumulation rate (SAR) at LR during these intervals, these conditions would have had to remain for decades to prevent opal removal from the top 2–3 cm of sediments and enable the deposition of sediment above.

Consequently, it is possible that export productivity was homogenous across the region during these intervals and the productivity conditions recorded in L5 and L6 did not differ from those during the deposition of the time-equivalent layers in the PM record. Instead, dysoxic/anoxic bottom-waters at LR containing high levels of dissolved silica led to the enhanced preservation of organic matter and carbonate fossil geochemical signatures, and the preservation of opaline skeletons of siliceous plankton. Consequently, the laminated layers at LR may offer rare insight into the productivity conditions that occur during insolation minimum (beige marls).

Within the L5, there is a difference between the Ba_{bio} and TOC concentrations in the upper and lower sections. The upper (lower) section displays reduced (increased) Ba_{bio} concentrations despite a higher (lower) TOC content. L6 also demonstrates lower Ba_{bio} concentration than L5 despite a higher TOC content, and lacks diatoms (H. Schrader, personal communication, 1995). This could have been the result of reduced SAR during the deposition of L6 and the upper section of L5 (Figure 2), which led to longer exposure of the upper sediments and consequently the dissolution of barium (Schoepfer et al., 2015) and opal. Another possibility, however, is that anaerobic degradation of organic matter took place during or soon after deposition of laminates L6 and L5. This may have led to barium mobilization and the destruction of siliceous organisms in L6 and the upper section of L5 (Brumsack, 1986; Van Os et al., 1991), whilst simultaneously enriching siliceous organisms and barium within the lower section of L5.

5.2. Paleoceanographic Conditions During the Deposition of the Beige and White Layers

The background conditions (CO_2 concentrations, global ice volume, and Northern Hemispheric summer insolation) during the deposition of the beige marls of the Trubi formation (~4.7–4.6 Ma) were remarkably similar to present day (Pagani et al., 2010; Tiedemann et al., 1994). This implies comparable climatic and paleoceanographic conditions at the time of their deposition to the contemporary eastern Mediterranean.

The maxima in Ti/Al in the beige layers (seen in both LR and PM records) indicates that the primary source of terrigenous material in these layers is aeolian, transported from the north African continent (Wehausen &

Brumsack, 1999). The relatively high $\delta^{18}O$ of the surface-waters (shown by both planktonic species; Figure 5) points to a lower influx of freshwater and/or lower surface-water temperatures compared to periods of gray marl deposition. This indicates increased aridity, reduced soil moisture and vegetation cover in North Africa resulting from the precession maxima (Larrasoaña et al., 2003). The reduced oxygen isotope gradient ($\Delta\delta^{18}O_{m\text{-}t}$) between the mixed-layer and thermocline (shown by *G. obliquus* and *N. acostaensis* $\delta^{18}O$, Figure 6) indicates enhanced ventilation of the eastern Mediterranean compared to insolation maxima and the deposition of the gray marls (Figures 7b and 7c). This is much like modern eastern Mediterranean conditions whereby vertical mixing is enhanced in the winter and surface-water stratification is confined to summer months (Krom et al., 1992).

The low levels of TOC and Ba_{bio} in the beige marls may point to reduced export productivity resulting from reduced nutrient availability in the photic zone (Schoepfer et al., 2015; Tribovillard et al., 2006; Van Os et al., 1994). The insight gained from the laminated layers, however, may challenge this interpretation. If L5 and L6 do indeed provide insight into the "true" productivity conditions during the deposition of the beige marls, export productivity may actually have been higher than previously acknowledged during these periods, but this signal is not typically preserved in the sedimentary record due to oxic bottom-waters caused by enhanced winter vertical mixing. In L6 and upper L5 (which coincide with precession maxima and the deposition of beige layers at PM), organic carbon levels are relatively high, pointing to significant export productivity. The minimum $CaCO_3$ values in both the beige marls and laminated layers at this time may indicate that calcareous organisms did not dominate primary productivity, but instead siliceous organisms played a significant role, as shown by the presence of siliceous skeletons and opal in the laminated layers.

Today, in addition to the "spring-bloom" that results from deep turbulent mixing during winter months, a summer bloom of "shade-flora" diatoms can occur in areas like the Mediterranean, which exhibit a strong seasonal thermocline and nutricline during the summer. Many diatom species are able to generate substantial production at depth beneath oligotrophic surface-waters (Kemp et al., 2000). These large, relatively slow growing diatom species, including *Thalassiothrix longissima* (a mat-forming species [i.e., Bodén & Backman, 1996]) and some *Coscinodiscus* spp., may represent "shade-flora" that have adapted to (a) grow in symbiosis with nitrogen-fixing cyanobacteria under low-light conditions and/or (b) regulate their buoyancy to move between a deep nutrient source and the euphotic zone (Kemp et al., 2000; Kemp & Villareal, 2013). During autumn and/or winter mixing, stratification will break down, causing as much, or in some cases even more, export production (the autumn "dump") than during the spring-bloom (Kemp et al., 2000). In particular, nutrients from intermediate layers can be upwelled, through isopycnal or diapycnal mixing, to the photic zone, thereby stimulating diatom production. Consequently, these laminated layers indicate that biomass blooms were not confined to late winter/early spring. Instead, these layers likely record two annual primary productivity blooms. The first of these is the winter/spring-bloom, dominated by calcareous organisms, when vertical turbulence fertilised the surface-ocean and deepened the mixed-layer, and/or Saharan dust fertilised the surface ocean (Rutten et al., 2000). The second of these is a summer bloom, dominated by siliceous "shade-flora." This theory may be supported by the presence of prasinophytes in L5 and L6 which today are found living together with diatoms in these deep-water algal communities related to nutrient-rich, cold waters (Jenkinson, 1986; Kimor & Wood, 1975; Prauss & Riegel, 1989; Sournia, 1982).

Finally, the white limestone layers correspond with increasing (white to gray layers) or decreasing (white to beige layers) input of riverine terrigenous material relative to aeolian terrigenous material (as shown by the Ti/Al record). These layers occur as Northern Hemisphere summer insolation is increasing (declining) from minimum (maximum) to maximum (minimum) values. The maximum $CaCO_3$ content suggests that calcareous primary producers (i.e., coccolithophores) dominated primary productivity which may point to oligotrophic conditions as these organisms thrive in low-nutrient environments (Malinverno et al., 2003; Ziveri et al., 2000). With decreasing summer insolation at this time, summer-stratification may not have been strong enough to allow for the summer "shade-flora" bloom, and therefore these layers represent transitional conditions in the eastern Mediterranean (Van Os et al., 1994), where calcareous organisms were the dominant primary producers.

5.3. Formation of the Gray Layers: Palaeoproductivity Versus Anoxia

The minimum Ti/Al values within the gray marls demonstrate a larger contribution of riverine sourced terrigenous material during these periods of maximum Northern Hemisphere summer insolation (65°N) (Lourens et al., 2001; Van Os et al., 1994; Wehausen & Brumsack, 1999) while the lowered oxygen isotope composition

of the mixed-layer and thermocline (as recorded by the *G. obliquus* and *N. acostaensis*) points to an enhanced input of ^{16}O-enriched monsoonal freshwater into the eastern Mediterranean basin caused by the precession index reaching minimum values (Emeis et al., 2003; Rohling et al., 2006; Rossignol-Strick, 1983, 1985) and/or elevated sea-surface temperatures. Furthermore, the decline in δ^{13}C of the mixed-layer and thermocline dwelling planktonic species, *G. obliquus* and *N. acostaensis*, also points to an enhanced supply of ^{12}C-enriched freshwater (Fontugne & Calvert, 1992), while the depleted δ^{13}C values of the benthic species, *C. italicus*, at this time likely reflects the lighter isotopic signature of the planktonic organisms reaching the sediment from the upper water column. Our planktonic δ^{18}O records show an enhanced oxygen isotope gradient between the mixed-layer and thermocline which point to a strong (summer) surface-water stratification resulting from the enhanced monsoonal input of freshwater (Rohling & Hilgen, 1991; Rossignol-Strick, 1983, 1985; van der Meer et al., 2007). The benthic δ^{18}O shows no obvious pattern in the gray layers, although the δ^{18}O values are higher than those of both planktonic species. This is not unique to the gray layers and is seen throughout the records, likely due to the lower temperatures and higher salinities that characterize deep-waters (Pierre, 1999).

Consequently, like previous sapropel research, these records show enhanced stratification during summer insolation maxima and gray marl deposition (Figure 7c). At this time, the TOC and Ba_{bio} concentration was also enhanced, but whether this is the result of increased productivity and/or enhanced preservation caused by anoxia needs to be explored here further.

The presence of benthic foraminifera throughout the gray marls of both records indicates that bottom-waters were not completely anoxic during their deposition (Rohling et al., 1993; Schmiedl et al., 2003). As the sediments of the Trubi formation were deposited in the mesopelagic zone (500–800 m), it is possible that there was still some ventilation at this depth, despite a significant reduction in vertical mixing, driven by the enhanced stratification (Figure 7c). Conditions at these sites may have been suboxic, with these benthic organisms representing low-oxygen tolerant species (Rohling et al., 1997). C_{org}/P_{total} and V/Sc ratios are also slightly higher in these layers, with values of the latter exceeding 9.1, indicating low bottom-water oxygen conditions which may have led to enhanced preservation of organic matter (e.g., Calvert & Pedersen, 1993; Emerson & Huested, 1991; Gallego-Torres et al., 2007).

Based on this information, it is possible that there was significant export productivity during the deposition of the gray layers, in combination with enhanced preservation (supported by well-preserved planktonic foraminifera in these samples [Figure S1 in the Supporting Information S1]). Enhanced preservation was likely caused by suboxic bottom-waters which were generated by reduced ventilation resulting from freshwater-induced stratification. This then led to the enhanced TOC and Ba_{bio} signature of these layers. The reduced surface-water salinity will have led to the shoaling of the pycnocline into the euphotic zone leading to the formation of a DCM and oligotrophic surface-waters (Rohling, 1991). The low levels of $CaCO_3$ and reduced flux of planktonic foraminifera at this time point to a significant drop in carbonate productivity in the upper ocean (Van Os et al., 1994). Consequently, primary productivity was likely dominated by siliceous "shade-flora," adapted to oligotrophic conditions (Kemp et al., 1999, 2000). The preservation of these opaline skeletons has been shown to be highly variable within sapropels (Kemp et al., 1999; Van Os et al., 1994) and the suboxic bottom-water conditions and silica undersaturation (as seen in the modern Mediterranean) at this site during the time of deposition of the gray marls may have prevented the preservation of siliceous organisms in our records. Despite the freshwater-induced stratification, some vertical mixing must have occurred during these periods to enable the survival of benthic organisms and to supply sufficient nutrients to the DCM for primary productivity. We argue, however, that without the deep winter mixing that occurs in the modern Mediterranean, two important processes which today contribute significantly to export productivity, will not have occurred: (a) the annual fertilisation of the upper water column that leads to the spring-bloom, and (b) the autumn "dump" of the slow-growing "shade-flora" produced in the DCM. Furthermore, the reduced influx of minerals and iron to the eastern Mediterranean, supplied by Saharan dust may have also affected nutrient availability in the surface-ocean (Foucault & Mélières, 2000; Larrasoaña et al., 2003). As a result of the sustained stratification and oligotrophic surface-waters, nutrients and minerals will have been heavily recycled within the nutricline.

While previous research suggests that export productivity was significantly enhanced during precession minima compared to other periods of the precession cycle (e.g., Calvert & Fontugne, 2001; Lourens et al., 1992; Wehausen & Brumsack, 1999), the laminated layers at LR contest this view. These layers may provide a "window" into the "true" productivity conditions during precession maxima (i.e., the deposition of the beige marls) and show that

export productivity was not significantly reduced compared to precession minima (i.e., the deposition of the gray marls). The enhanced organic matter content of the gray marls is influenced by both increased export productivity and enhanced preservation caused by lower bottom-water oxygenation resulting from freshwater-induced stratification.

6. Conclusions

- The laminated layers in the LR record are thought to be caused by a local depression at this site which led to the intermittent presence of a stagnant dysoxic/anoxic pool. This resulted in the preservation of organic matter and siliceous opaline skeletons during these periods.
- The productivity signal preserved in L5, L6, and the gray marls offers rare insight into productivity conditions in the eastern Mediterranean during precession maximum (beige marls) and precession minimum (gray marls). The productivity signal preserved in the beige marls offers particularly valuable insight into conditions during precession maximum, as, during these periods, bottom-waters are typically well-ventilated and undersaturated in silica, leading to poor preservation of organic matter and siliceous materials.
- The productivity conditions in this region during beige layer deposition are likely to be comparable to those of the modern eastern Mediterranean. The large seasonal contrast in vertical mixing of the upper water column during these periods plays an important role in export productivity. Enhanced deep-water mixing during winter and spring leads to a spring-bloom, while the summer-stratification induced DCM leads to a "shade-flora" bloom which is deposited to the sea-floor in autumn during stratification break-down.
- During gray marl deposition, increased freshwater-influx into the Mediterranean (forced by precession minimum) led to enhanced, prolonged eastern Mediterranean stratification and DCM formation, resulting in export productivity dominated by "shade-flora." In addition to enhanced export productivity during these intervals, suboxic bottom-water conditions, caused by freshwater-forced stratification, also played an important role in preserving the geochemical signals in the gray marls.
- While the preservation of microfossils and geochemical signals in eastern Mediterranean sedimentary sequences is typically higher during precession minimum than precession maximum, the enhanced preservation in both laminated layers indicate that export productivity may not have been significantly lower during precession maximum compared to periods of precession minimum.

Data Availability Statement

All data generated for this study are archived and publicly available via the Mendeley Data repository online (Cutmore et al., 2023).

Acknowledgments
Samples would not have been collected without the aid of F.J. Hilgen, W. Krijgsman and C. E. Duermeijer. For technical support with the geochemical, micropaleontological, and stable isotope analyses we thank P. Anten, D. van de Meent, A. van Dijk, G. Nobbe, H. de Waard, T. Zalm, T. Broer, G. J. van het Veld and G. Ittman. We also thank L. Pronk and L. Stille for picking and analyzing the planktonic and benthic foraminiferal specimen for their stable isotope composition. Special thanks goes to H. Schrader and L. Beaufort, whom carried out preliminary studies on the diatom and nannofossil contents of the samples, respectively. This long-standing study was partly funded by the Netherlands Organization for Scientific Research (NWO), through the PIONEER program of F.J. Hilgen, VIDI program of L. J. Lourens, and the Netherlands Earth System Science Centre (NESSC).

References

Algeo, T. J., & Lyons, T. W. (2006). Mo–total organic carbon covariation in modern anoxic marine environments: Implications for analysis of paleoredox and paleohydrographic conditions. *Paleoceanography & Paleoclimatology*, *21*, 1–23. https://doi.org/10.1029/2004PA001112

Azov, Y. (1986). Seasonal patterns of phytoplankton productivity and abundance in near-shore oligotrophic waters of the Levant Basin (Mediterranean). *Journal of Plankton Research*, *8*(1), 41–53. https://doi.org/10.1093/plankt/8.1.41

Azrieli-Tala, I., Matthews, A., Bar-Matthews, M., Almogi-Labin, A., Vance, D., Archer, C., & Teutsch, N. (2014). Evidence from molybdenum and iron isotopes and molybdenum–uranium covariation for sulphidic bottom waters during Eastern Mediterranean sapropel S1 formation. *Earth and Planetary Science Letters*, *393*, 231–242. https://doi.org/10.1016/j.epsl.2014.02.054

Beltran, C., Sicre, M.-A., Ohneiser, C., & Sainz, M. (2021). A composite Pliocene record of sea surface temperature in the central Mediterranean (Capo Rossello composite section – South Sicily). *Sedimentary Geology*, *420*, 1–8. https://doi.org/10.1016/j.sedgeo.2021.105921

Berger, A., & Loutre, M. F. (1991). Insolation values for the climate of the last 10 million years. *Quaternary Science Reviews*, *10*(4), 297–317. https://doi.org/10.1016/0277-3791(91)90033-Q

Berggren, W. A., & Amdurer, M. (1973). *Late Paleogene (Oligocene) and neogene planktonic foraminiferal biostratigraphy of the Atlantic Ocean (Lat. 30 Degrees N to Lat. 30 Degrees S)* (Institutional Technical Report) (pp. 73–34). Woods Hole Oceanographic Institution Mass.

Berman, T., Azov, Y., & Townsand, D. W. (1984). Understanding oligotrophic oceans: Can the eastern Mediterranean be a useful model? In O. Holm-Hansen, L. Bolis, & R. Gilles (Eds.), *Marine phytoplankton and productivity, Lecture notes on coastal and estuarine studies* (pp. 101–111). Springer Verlag. https://doi.org/10.1007/978-3-662-02401-0_9

Berman, T., Townsand, D. W., El-Sayed, S. Z., Trees, C. C., & Azov, Y. (1984). Optical transparency, chlorophyll and primary productivity in the Eastern Mediterranean near the Israeli coast. *Oceanologica Acta*, *7*, 367–372.

Bishop, J. K. B. (1988). The barite-opal-organic carbon association in oceanic particulate matter. *Nature*, *332*(6162), 341–343. https://doi.org/10.1038/332341a0

Björklund, K. R., & De Ruiter, R. (1987). Radiolarian preservation in Eastern Mediterranean anoxic sediments. *Marine Geology*, *75*(1–4), 271–281. https://doi.org/10.1016/0025-3227(87)90109-5

Boalch, G. T., & Parke, M. (1971). The Prasinophycean genera (Chlorophyta) possibly related to fossil genera, in particular the genus Tasmanites. In *Proceedings of the II planktonic conference, Roma 1970* (pp. 99–105).
Bodén, P., & Backman, J. (1996). A laminated sediment sequence from the northern North Atlantic Ocean and its climatic record. *Geology*, *24*(6), 507–510. https://doi.org/10.1130/0091-7613(1996)024<0507:ALSSFT>2.3.CO;2
Brenner, S., Rozentraub, Z., Bishop, J., & Krom, M. (1991). The mixed-layer/thermocline cycle of a persistent warm core eddy in the eastern Mediterranean. *Dynamics of Atmospheres and Oceans*, *15*(3–5), 457–476. https://doi.org/10.1016/0377-0265(91)90028-E
Brolsma, M. J. (1978). Quantitative foraminiferal analysis and environmental interpretation of the Pliocene and topmost Miocene on the south coast of Sicily. *Utrecht Micropaleontological Bulletins*, *18*. 159 pp.
Brumsack, H. J. (1986). The inorganic geochemistry of Cretaceous black shales (DSDP Leg 41) in comparison to modern upwelling sediments from the Gulf of California. *Geological Society, London Special Publications*, *21*(1), 447–462. https://doi.org/10.1144/GSL.SP.1986.021.01.30
Burnett, W. C. (1977). Geochemistry and origin of phosphorite deposits from off Peru and Chile. *GSA Bulletin*, *88*(6), 813–823. https://doi.org/10.1130/0016-7606(1977)88<813:GAOOPD>2.0.CO;2
Calvert, S. E. (1983). Geochemistry of Pleistocene sapropels and associated sediments from the eastern Mediterranean. *Oceanologica Acta*, *6*, 255–267.
Calvert, S. E., & Fontugne, M. R. (2001). On the late Pleistocene-Holocene sapropel record of climatic and oceanographic variability in the eastern Mediterranean. *Palaeoceanography*, *16*(1), 78–94. https://doi.org/10.1029/1999PA000488
Calvert, S. E., Nielsen, B., & Fontugne, M. R. (1992). Evidence from nitrogen isotope ratios for enhanced productivity during formation of eastern Mediterranean sapropels. *Nature*, *359*(6392), 223–225. https://doi.org/10.1038/359223a0
Calvert, S. E., & Pedersen, T. F. (1993). Geochemistry of recent oxic and anoxic marine sediments: Implications for the geological record. *Marine Geology*, *113*(1–2), 67–88. https://doi.org/10.1016/0025-3227(93)90150-T
Canfield, D. E. (1994). Factors influencing organic carbon preservation in marine sediments. *Chemical Geology*, *114*(3–4), 315–329. https://doi.org/10.1016/0009-2541(94)90061-2
Canfield, D. E., Lyons, T. W., & Raiswell, R. (1996). A model for iron deposition to euxinic Black Sea sediments. *American Journal of Science*, *296*(7), 818–834. https://doi.org/10.2475/ajs.296.7.818
Castradori, D. (1993). Calcareous nannofossils and the origin of eastern Mediterranean sapropels. *Palaeoceanography and Palaeoclimatology*, *8*(4), 459–471. https://doi.org/10.1029/93PA00756
Corfield, R. M., & Cartlidge, J. (1992). Oceanographic and climatic implications of the Paleocene carbon isotope maximum. *Terra Nova*, *4*, 443–455. https://doi.org/10.1111/j.1365-3121.1992.tb00579.x
Corselli, C., Principato, M. S., Maffioli, P., & Crudelli, D. (2002). Changes in planktonic assemblages during sapropel S5 deposition: Evidence from Urania Basin area, eastern Mediterranean. *Paleoceanography*, *17*(3), 1–30. https://doi.org/10.1029/2000PA000536
Crusius, J., Calvert, S., Pedersen, T., & Sage, D. (1996). Rhenium and molybdenum enrichments in sediments as indicators of oxic, suboxic and sulfidic conditions of deposition. *Earth and Planetary Science Letters*, *145*(1–4), 65–78. https://doi.org/10.1016/S0012-821X(96)00204-X
Cutmore, A., Lourens, L., & de Lange, G. (2023). Mid-Pliocene nannofossil, isotope and geochemical records from Lido Rossello & Punta di Maiata, SW Sicily [Dataset]. Mendeley Data, V1. https://doi.org/10.17632/zcxfm4dv6b.1
De Lange, G. J., Middelburg, J. J., Van der Weijden, C. H., Catalano, G., Luther, G. W., III, Hydes, D. J., et al. (1990). Composition of anoxic hypersaline brines in the Tyro and Bannock basins, eastern Mediterranean. *Marine Chemistry*, *31*(1–3), 63–88. https://doi.org/10.1016/0304-4203(90)90031-7
Dehairs, F., Chesselet, R., & Jedwab, J. (1980). Discrete suspended particles of barite and the barium cycle in the open ocean. *Earth and Planetary Science Letters*, *49*(2), 528–550. https://doi.org/10.1016/0012-821X(80)90094-1
De Visser, J. P., Ebbing, J. H. J., Gudjonsson, L., Hilgen, F. J., Jorissen, F. J., Verhallen, P. J. J. M., & Zevenboom, D. (1989). The origin of rhythmic bedding in the Pliocene Trubi Formation of Sicily, southern Italy. *Palaeogeography, Palaeoclimatology, Palaeoecology*, *69*, 45–66. https://doi.org/10.1016/0031-0182(89)90155-7
Dowidar, N. M. (1984). Phytoplankton biomass and primary productivity of the south-eastern Mediterranean. *Deep Sea Research Part A. Oceanographic Research Papers*, *31*(6–8), 983–1000. https://doi.org/10.1016/0198-0149(84)90052-9
Emeis, K.-C., Schulz, H., Struck, U., Rossignol-Strick, M., Erlenkeuser, H., Howell, M. W., et al. (2003). Eastern Mediterranean surface water temperatures and δ18O composition during deposition of sapropels in the late Quaternary. *Palaeoceanography and Palaeoclimatology*, *18*, 1–18. https://doi.org/10.1029/2000PA000617
Emerson, S., & Huested, S. (1991). Ocean anoxia and the concentrations of molybdenum and vanadium in seawater. *Marine Chemistry*, *34*(3–4), 177–196. https://doi.org/10.1016/0304-4203(91)90002-E
Erba, E. (1991). Deep mid-water bacterial mats from anoxic basins of the Eastern Mediterranean. *Marine Geology*, *100*(1–4), 83–101. https://doi.org/10.1016/0025-3227(91)90226-t
Fairbanks, R. G., Sverdlove, M., Free, R., Wiebe, P. H., & Bé, A. W. H. (1982). Vertical distribution and isotopic fractionation of living planktonic foraminifera from the Panama Basin. *Nature*, *298*(5877), 841–844. https://doi.org/10.1038/298841a0
Fontugne, M. R., & Calvert, S. E. (1992). Late Pleistocene variability of the carbon isotopic composition of organic matter in the eastern Mediterranean: Monitor of changes in carbon sources and atmospheric CO2 concentrations. *Paleoceanography and Paleoclimatology*, *7*, 1–20. https://doi.org/10.1029/91PA02674
Foucault, A., & Mélières, F. (2000). Palaeoclimatic cyclicity in central Mediterranean Pliocene sediments: The mineralogical signal. *Palaeogeography, Palaeoclimatology, Palaeoecology*, *158*(3–4), 311–323. https://doi.org/10.1016/S0031-0182(00)00056-0
Froelich, P. N., Arthur, M. A., Burnett, W. C., Deakin, M., Hensley, V., Jahnke, R., et al. (1988). Early diagenesis of organic matter in Peru continental margin sediments: Phosphorite precipitation. *Marine Geology*, *80*(3–4), 309–343. https://doi.org/10.1016/0025-3227(88)90095-3
Gallego-Torres, D., Martínez-Ruiz, F., Paytan, A., Jiménez-Espejo, F. J., & Ortega-Huertas, M. (2007). Pliocene–Holocene evolution of depositional conditions in the eastern Mediterranean: Role of anoxia vs. productivity at time of sapropel deposition. *Palaeogeography, Palaeoclimatology, Palaeoecology*, *246*(2–4), 424–439. https://doi.org/10.1016/j.palaeo.2006.10.008
Guy-Ohlson, D. (1988). Developmental stages in the life cycle of Mesozoic Tasmanites. *Botanica Marina*, *31*(5), 447–456. https://doi.org/10.1515/botm.1988.31.5.447
Hemleben, C., Spindler, M., & Anderson, O. R. (1989). Trophic activity and nutrition. In C. Hemleben, M. Spindler, & O. R. Anderson (Eds.), *Modern planktonic foraminifera* (pp. 112–138).
Hilgen, F. J. (1991). Extension of the astronomically calibrated (polarity) time scale to the Miocene/Pliocene boundary. *Earth and Planetary Science Letters*, *107*(2), 349–368. https://doi.org/10.1016/0012-821X(91)90082-S
Hilgen, F. J., Abdul Aziz, H., Krijgsman, W., Raffi, I., & Turco, E. (2003). Integrated stratigraphy and astronomical tuning of the Serravallian and lower Tortonian at Monte dei Corvi (Middle–Upper Miocene, northern Italy). *Palaeogeography, Palaeoclimatology, Palaeoecology*, *199*(3–4), 229–264. https://doi.org/10.1016/S0031-0182(03)00505-4

Hilgen, F. J., & Langereis, C. G. (1989). Periodicities of CaCO3 cycles in the Pliocene of Sicily: Discrepancies with the quasi-periods of the Earth's orbital cycles? *Terra Nova*, *1*(5), 409–415. https://doi.org/10.1111/j.1365-3121.1989.tb00401.x

Jenkinson, I. R. (1986). Oceanographic implications of non-Newtonian properties found in phytoplankton cultures. *Nature*, *323*(6087), 435–437. https://doi.org/10.1038/323435a0

Kemp, A. E. S., Pearce, R. B., Koizumi, I., Pike, J., & Rance, S. J. (1999). The role of mat-forming diatoms in the formation of Mediterranean sapropels. *Nature*, *398*(6722), 57–61. https://doi.org/10.1038/18001

Kemp, A. E. S., Pike, J., Pearce, R. B., & Lange, C. B. (2000). The "Fall dump" — A new perspective on the role of a "shade flora" in the annual cycle of diatom production and export flux. *Deep Sea Research Part II: Topical Studies in Oceanography*, *47*(9–11), 2129–2154. https://doi.org/10.1016/S0967-0645(00)00019-9

Kemp, A. E. S., & Villareal, T. A. (2013). High diatom production and export in stratified waters – A potential negative feedback to global warming. *Progress in Oceanography*, *119*, 4–23. https://doi.org/10.1016/j.pocean.2013.06.004

Kimor, B., & Wood, E. J. F. (1975). A plankton study in the eastern Mediterranean Sea. *Marine Biology*, *29*(4), 321–333. https://doi.org/10.1007/BF00388852

Krom, M. D., Brenner, S., Kress, N., Neori, A., & Gordon, L. I. (1992). Nutrient dynamics and new production in a warm-core eddy from the Eastern Mediterranean Sea. *Deep Sea Research Part A. Oceanographic Research Papers*, *39*(3–4), 467–480. https://doi.org/10.1016/0198-0149(92)90083-6

Krom, M. D., Kress, N., Brennen, S., & Gordon, L. I. (1991). Gordon phosphorus limitation of primary productivity in the eastern Mediterranean Sea. *Limnology and Oceanography*, *36*(3), 424–432. https://doi.org/10.4319/lo.1991.36.3.0424

Kroopnick, P. M. (1985). The distribution of 13C of ΣCO2 in the world oceans. *Deep Sea Research Part A. Oceanographic Research Papers*, *32*(1), 57–84. https://doi.org/10.1016/0198-0149(85)90017-2

Kullenberg, B. (1952). *On the salinity of water contained in marine sediments*. In *Mediterranean Oceanographic Institute of Goteborg* (Vol. 21, pp. 1–38). Elanders boktr.

Lacombe, H., & Tchernia, P. (1972). Caractères hydrologiques et circulation des eaux en Méditerranée. In D. J. Stanley (Ed.), *The Mediterranean Sea* (pp. 25–36). Dowden, Hutchinson and Ross.

Larrasoaña, J. C., Roberts, A. P., Rohling, E. J., Winklhofer, M., & Wehausen, R. (2003). Three million years of monsoon variability over the northern Sahara. *Climate Dynamics*, *21*(7–8), 689–698. https://doi.org/10.1007/s00382-003-0355-z

Laskar, J., Joutel, F., & Boudin, F. (1993). Orbital, precessional, and insolation quantities for the Earth from -20 Myr to +10 Myr. *Astronomy and Astrophysics*, *270*, 522–533.

Lourens, L. J., Antonarakou, A., Hilgen, F. J., Van Hoof, A. A. M., Vergnaud-Grazzini, C., & Zachariasse, W. J. (1996). Evaluation of the Plio-Pleistocene astronomical timescale. *Palaeoceanography and Palaeoclimatology*, *11*(4), 391–413. https://doi.org/10.1029/96PA01125

Lourens, L. J., Hilgen, F. J., Gudjonsson, L., & Zachariasse, W. J. (1992). Late Pliocene to early Pleistocene astronomically forced sea surface productivity and temperature variations in the Mediterranean. *Marine Micropaleontology*, *19*(1–2), 49–78. https://doi.org/10.1016/0377-8398(92)90021-B

Lourens, L. J., Wehausen, R., & Brumsack, H. J. (2001). Geological constraints on tidal dissipation and dynamical ellipticity of the Earth over the past three million years. *Nature*, *409*(6823), 1029–1033. https://doi.org/10.1038/35059062

Lyons, T. W., & Severmann, S. (2006). A critical look at iron paleoredox proxies: New insights from modern euxinic marine basins. *Geochimica et Cosmochimica Acta*, *70*(23), 5698–5722. https://doi.org/10.1016/j.gca.2006.08.021

Malinverno, E., Corselli, C., Ziveri, P., De Lange, G., & Hübner, A. (2003). Coccolithophorid export production and fluxes in the Ionian Basin, eastern Mediterranean. *Journal of Geophysical Research*, *108*, 1–16.

Malinverno, E., Maffioli, P., Corselli, C., & De Lange, G. (2014). Present-day fluxes of coccolithophores and diatoms in the pelagic Ionian Sea. *Journal of Marine Systems*, *132*, 13–27. https://doi.org/10.1016/j.jmarsys.2013.12.009

Marullo, S., Santoleri, R., Malanotte-Rizzoli, P., & Bergamasco, A. (1999). The sea surface temperature field in the eastern Mediterranean from advanced very high resolution radiometer (AVHRR) data: Part I. Seasonal variability. *Journal of Marine Systems*, *20*(1–4), 63–81. https://doi.org/10.1016/S0924-7963(98)00071-2

Müller, P. J., & Schneider, R. (1993). An automated leaching method for the determination of opal in sediments and particulate matter. *Deep Sea Research Part I: Oceanographic Research Papers*, *40*(3), 425–444. https://doi.org/10.1016/0967-0637(93)90140-X

Nijenhuis, I. A., Bosch, H.-J., Sinninghe Damste, J. S., Brumsack, H.-J., & De Lange, G. J. (1999). Organic matter and trace element rich sapropels and black shales: A geochemical comparison. *Earth and Planetary Science Letters*, *169*(3–4), 277–290. https://doi.org/10.1016/S0012-821X(99)00083-7

Olausson, E. (1961). Studies of deep sea cores. *Reports of the Swedish Deep-Sea Expedition*, *8*, 337–391.

Pagani, M., Liu, Z., La Riviere, J., & Ravelo, A. C. (2010). High Earth-system climate sensitivity determined from Pliocene carbon dioxide concentrations. *Nature Geoscience*, *3*(1), 27–30. https://doi.org/10.1038/ngeo724

Parke, M., & Hartog-Adams, I. (1965). Three species of Halosphaera. *Journal of the Marine Biological Association of the United Kingdom*, *45*(2), 525–536. https://doi.org/10.1017/S0025315400054990

Parker, F. L. (1973). Living planktonic foraminifera from the Gulf of California. *Journal of Foraminiferal Research*, *3*(2), 70–77. https://doi.org/10.2113/gsjfr.3.2.70

Passier, H. F., Bosch, H.-J., Nijenhuis, I. A., Lourens, L. J., Böttcher, M. E., Leenders, A., et al. (1999). Sulphidic Mediterranean surface waters during Pliocene sapropel formation. *Nature*, *397*(6715), 146–149. https://doi.org/10.1038/16441

Paytan, A., & Griffiths, E. M. (2007). Marine barite: Recorder of variations in ocean export productivity. *Deep Sea Research Part II: Topical Studies in Oceanography*, *54*(5–7), 687–705. https://doi.org/10.1016/j.dsr2.2007.01.007

Pedersen, T. F., & Calvert, S. E. (1990). Anoxia vs. productivity: What controls the formation of organic-rich sediments and sedimentary rocks? *American Association of Petroleum Geologists Bulletin*, *74*, 454–466. https://doi.org/10.1306/0C9B232B-1710-11D7-8645000102C1865D

Pierre, C. (1999). The oxygen and carbon isotope distribution in the Mediterranean water masses. *Marine Geology*, *153*(1–4), 41–55. https://doi.org/10.1016/S0025-3227(98)00090-5

Prauss, M., & Riegel, W. (1989). Evidence from phytoplankton associations for causes of black shale formation in epicontinental seas. *Neues Jahrbuch für Geologie und Paläontologie*, *11*, 671–682. https://doi.org/10.1127/njgpm/1989/1989/671

Pujol, C., & Vergnaud-Grazzini, C. (1995). Distribution patterns of live planktic foraminifers as related to regional hydrography and productive systems of the Mediterranean Sea. *Marine Micropaleontology*, *25*(2–3), 187–217. https://doi.org/10.1016/0377-8398(95)00002-I

Ravelo, A. C., & Fairbanks, R. G. (1992). Oxygen isotopic composition of multiple species of planktonic foraminifera: Recorders of the modern photic zone temperature gradient. *Paleoceanography and Paleoclimatology*, *7*(6), 815–831. https://doi.org/10.1029/92PA02092

Reichart, G. J., Lourens, L. J., & Zachariasse, W. J. (1998). Temporal variability in the northern Arabian Sea oxygen minimum zone (OMZ) during the last 225,000 years. *Palaeoceanography and Palaeoclimatology*, *13*(6), 607–621. https://doi.org/10.1029/98PA02203

Rögl, F., & Steininger, F. F. (1983). Vom Zerfall der Tethys zu Mediterran und Paratethys. Die neogene Paläogeographie und Palinspastik des zirkum-mediterranen Raumes. *Annalen des Naturhistorischen Museums in Wien A*, *85*, 135–163.

Rohling, E. J. (1991). A simple two-layered model for shoaling of the eastern Mediterranean pycnocline due to glacio-eustatic sea level lowering. *Paleoceanography and Paleoclimatology*, *6*(4), 537–541. https://doi.org/10.1029/91PA01328

Rohling, E. J. (1994). Review and new aspects concerning the formation of eastern Mediterranean sapropels. *Marine Geology*, *122*(1–2), 1–28. https://doi.org/10.1016/0025-3227(94)90202-X

Rohling, E. J., Cane, T. R., Cooke, S., Sprovieri, M., Bouloubassi, I., Emeis, K. C., et al. (2002). African monsoon variability during the previous interglacial maximum. *Earth and Planetary Science Letters*, *202*(1), 61–75. https://doi.org/10.1016/S0012-821X(02)00775-6

Rohling, E. J., & Gieskes, W. W. C. (1989). Late Quaternary changes in Mediterranean intermediate water density and formation rate. *Paleoceanography*, *4*(5), 531–545. https://doi.org/10.1029/PA004i005p00531

Rohling, E. J., & Hilgen, F. J. (1991). The eastern Mediterranean climate at times of sapropel formation: A review. *Geologien Mijnbouw*, *70*, 253–264.

Rohling, E. J., Hopmans, E. C., & Sinninghe Damsté, J. S. (2006). Water column dynamics during the last interglacial anoxic event in the Mediterranean (sapropel S5). *Paleoceanography and Paleoclimatology*, *21*(2), 1–8. https://doi.org/10.1029/2005PA001237

Rohling, E. J., Jorissen, F. J., & De Stigter, H. C. (1997). 200 Year interruption of Holocene sapropel formation in the Adriatic Sea. *Journal of Micropalaeontology*, *16*(2), 97–108. https://doi.org/10.1144/jm.16.2.97

Rohling, E. J., Jorissen, F. J., Vergnaud Grazzini, C., & Zachariasse, W. J. (1993). Northern Levantine and Adriatic Quaternary planktic foraminifera; Reconstruction of paleoenvironmental gradients. *Marine Micropaleontology*, *21*(1–3), 191–218. https://doi.org/10.1016/0377-8398(93)90015-P

Rossignol-Strick, M. (1983). African monsoons, an immediate climate response to orbital insolation. *Nature*, *304*(5921), 46–49. https://doi.org/10.1038/304046a0

Rossignol-Strick, M. (1985). Mediterranean Quaternary sapropels, an immediate response of the African monsoon to variation of insolation. *Palaeogeography, Palaeoclimatology, Palaeoecology*, *49*(3–4), 237–263. https://doi.org/10.1016/0031-0182(85)90056-2

Rossignol-Strick, M., Nesteroff, W., Olive, P., & Vergnaud-Grazzini, C. (1982). After the deluge: Mediterranean stagnation and sapropel formation. *Nature*, *295*(5845), 105–110. https://doi.org/10.1038/295105a0

Roussenov, V., Stanev, E., Artale, V., & Pinardi, N. (1995). A seasonal model of the Mediterranean Sea general circulation. *Journal of Geophysical Research*, *100*(C7), 13515–13538. https://doi.org/10.1029/95JC00233

Rutten, A., de Lange, G. J., Ziveri, P., Thomson, J., van Santvoort, P. J. M., Colley, S., & Corselli, C. (2000). Recent terrestrial and carbonate fluxes in the pelagic eastern Mediterranean; A comparison between sediment trap and surface sediment. *Palaeogeography, Palaeoclimatology, Palaeoecology*, *158*(3–4), 197–213. https://doi.org/10.1016/s0031-0182(00)00050-x

Sachs, J. P., & Repeta, D. J. (1999). Oligotrophy and nitrogen fixation during eastern Mediterranean sapropel events. *Science*, *286*(5449), 2485–2488. https://doi.org/10.1126/science.286.5449.2485

Scheiderich, K., Zerkle, A. L., Helz, G. R., Farquhar, J., & Walker, R. J. (2010). Molybdenum isotope, multiple sulfur isotope, and redox-sensitive element behavior in early Pleistocene Mediterranean sapropels. *Chemical Geology*, *279*(3–4), 134–144. https://doi.org/10.1016/j.chemgeo.2010.10.015

Schmiedl, G., Mitschele, A., Beck, S., Emeis, K.-C., Hemleben, C., Schulz, H., et al. (2003). Benthic foraminiferal record of ecosystem variability in the eastern Mediterranean Sea during times of sapropel S5 and S6 deposition. *Palaeogeography, Palaeoclimatology, Palaeoecology*, *190*, 139–164. https://doi.org/10.1016/s0031-0182(02)00603-x

Schoepfer, S. D., Shen, J., Wei, H., Tyson, R. V., Ingall, E., & Algeo, T. J. (2015). Total organic carbon, organic phosphorus, and biogenic barium fluxes as proxies for paleomarine productivity. *Earth-Science Reviews*, *149*, 23–52. https://doi.org/10.1016/j.earscirev.2014.08.017

Scrivner, A., Vance, D., & Rohling, E. J. (2004). New neodymium isotope data quantify Nile involvement in Mediterranean anoxic episodes. *Geology*, *32*(7), 565–568. https://doi.org/10.1130/G20419.1

Shackleton, N. J. (1985). Oceanic carbon isotope constraints on oxygen and carbon dioxide in the Cenozoic atmosphere. In E. T. Sundquist & W. S. Broecker (Eds.), *The carbon cycle and atmospheric CO_2: Natural variations Archean to Present: Proceedings of the Chapman conference on natural variations in carbon dioxide and the carbon cycle* (pp. 412–417). AGU. https://doi.org/10.1029/GM032p0412

Sournia, A. (1982). Is there a shade flora in the marine plankton? *Journal of Plankton Research*, *4*(2), 391–399. https://doi.org/10.1093/plankt/4.2.391

Sprovieri, R., & Hasegawa, S. (1990). Plio-pleistocene benthic foraminifer stratigraphic distribution in the deep-sea record of the Tyrrhenian Sea (Odp Leg 107). *Proceedings of the Ocean Drilling Program, Scientific Results*, *107*, 429–459.

Srinivasan, M. S., & Kennett, J. P. (1976). Evolution and phenotypic variation in the Late Cenozoic Neogloboquadrina dutertrei plexus. In Y. Takayanagi & T. Saito (Eds.), *Progress in micropaleontology: Selected papers in honor of prof. Kiyoshi Asano* (pp. 329–354). Micropaleontology Press.

Thunell, R. C. (1979). Pliocene - Pleistocene paleotemperature and paleosalinity history of the Mediterranean Sea: Results from DSDP sites 125 and 132. *Marine Micropaleontology*, *4*, 173–187. https://doi.org/10.1016/0377-8398(79)90013-6

Tiedemann, R., Sarnthein, M., & Shackleton, N. J. (1994). Astronomic timescale for the Pliocene Atlantic δ18O and dust flux records of Ocean Drilling Program site 659. *Palaeoceanography and Palaeoclimatology*, *9*(4), 619–638. https://doi.org/10.1029/94PA00208

Tribovillard, N., Algeo, T. J., Lyons, T., & Riboulleau, A. (2006). Trace metals as paleoredox and paleoproductivity proxies: An update. *Chemical Geology*, *232*(1–2), 12–32. https://doi.org/10.1016/j.chemgeo.2006.02.012

van der Meer, M. T. J., Baas, M., Rijpstra, W. I. C., Marino, G., Rohling, E. J., Sinninghe Damsté, J. S., & Schouten, S. (2007). Hydrogen isotopic compositions of long-chain alkenones record freshwater flooding of the Eastern Mediterranean at the onset of sapropel deposition. *Earth and Planetary Science Letters*, *262*(3–4), 594–600. https://doi.org/10.1016/j.epsl.2007.08.014

Van Os, B. J. H., Lourens, L. J., Hilgen, F. J., De Lange, G. J., & Beaufort, L. (1994). The formation of Pliocene sapropels and carbonate cycles in the Mediterranean: Diagenesis, dilution, and productivity. *Palaeoceanography and Palaeoclimatology*, *9*(4), 601–617. https://doi.org/10.1029/94PA00597

Van Os, B. J. H., Middelburg, J. J., & de Lange, G. J. (1991). Possible diagenetic mobilization of barium in sapropelic sediment from the eastern Mediterranean. *Marine Geology*, *100*(1–4), 125–136. https://doi.org/10.1016/0025-3227(91)90229-w

Varkitzi, I., Psarra, S., Assimakopoulou, G., Pavlidou, A., Krasakopoulou, E., Velaoras, D., et al. (2020). Phytoplankton dynamics and bloom formation in the oligotrophic eastern Mediterranean: Field studies in the Aegean, Levantine and Ionian seas. *Deep Sea Research Part II: Topical Studies in Oceanography*, *171*, 1–16. https://doi.org/10.1016/j.dsr2.2019.104662

Vergnaud-Grazzini, C., Ryan, W. B. F., & Cita, M. B. (1977). Stable isotopic fractionation, climate change and episodic stagnation in the eastern Mediterranean during the late Quaternary. *Marine Micropaleontology*, *2*, 353–370. https://doi.org/10.1016/0377-8398(77)90017-2

Wall, D., Dale, B., Lohmann, G. P., & Smith, W. K. (1977). The environmental and climatic distribution of dinoflagellate cysts in modern marine sediments from regions in the North and South Atlantic Oceans and adjacent seas. *Marine Micropaleontology*, *2*, 121–200. https://doi.org/10.1016/0377-8398(77)90008-1

Wehausen, R., & Brumsack, H.-J. (1999). Cyclic variations in the chemical composition of eastern Mediterranean Pliocene sediments: A key for understanding sapropel formation. *Marine Geology*, *153*(1–4), 161–176. https://doi.org/10.1016/S0025-3227(98)00083-8

Williams, D. F., Bé, A. W. H., & Fairbanks, R. G. (1979). Seasonal oxygen isotopic variations in living planktonic foraminifera off Bermuda. *Science*, *206*(4417), 447–449. https://doi.org/10.1126/science.206.4417.447

Wu, J., Filippidi, A., Davies, G. R., & de Lange, G. J. (2018). Riverine supply to the eastern Mediterranean during last interglacial sapropel S5 formation: A basin-wide perspective. *Chemical Geology*, *485*, 74–89. https://doi.org/10.1016/j.chemgeo.2018.03.037

Wüst, G. (1960). On the vertical circulation of the Mediterranean Sea. *Journal of Geophysical Research*, *66*(10), 3261–3271. https://doi.org/10.1029/JZ066i010p03261

Zachariasse, W. J., Riedel, W. R., Sanfilippo, A., Schmidt, R. R., Brolsma, M. J., Schrader, H. J., et al. (1978). Micropaleontological counting methods and techniques: An exercise on an eight metres section of the lower Pliocene of Capo Rossello, Sicily. *Utrecht Micropaleontological Bulletins*, *17*, 1–264.

Ziveri, P., Rutten, A., De Lange, G., Thomson, J., & Corselli, C. (2000). Present-day coccolith fluxes recorded in central eastern Mediterranean sediment traps and surface sediments. *Palaeogeography, Palaeoclimatology, Palaeoecology*, *158*(3–4), 175–195. https://doi.org/10.1016/S0031-0182(00)00049-3